Bioorganic & Medicinal Chemistry Letters 21 (2011) 1385–1389

Contents lists available at ScienceDirect

Bioorganic & Medicinal Chemistry Letters

journal homepage: www.elsevier.com/locate/bmcl

Synthesis and anti-migrative evaluation of moverastin derivatives

Masato Sawada [a,†], Shin-ichiro Kubo [b,†], Koji Matsumura [b], Yasushi Takemoto [a], Hiroki Kobayashi [a], Etsu Tashiro [a], Takeshi Kitahara [b], Hidenori Watanabe [b,*], Masaya Imoto [a,*]

[a] Department of Biosciences and Informatics, Faculty of Science and Technology, Keio University, 3-14-1 Hiyoshi, Kohoku-ku, Yokohama 223-8522, Japan
[b] Graduate School of Agricultural and Life Sciences, The University of Tokyo, 1-1-1 Yayoi, Bunkyo-ku, Tokyo 113-8657, Japan

ARTICLE INFO

Article history:
Received 6 December 2010
Revised 6 January 2011
Accepted 7 January 2011
Available online 11 January 2011

Keywords:
Cell migration
Chemical synthesis
UTKO1

ABSTRACT

Cell migration of tumor cells is essential for invasion of the extracellular matrix and for cell dissemination. Inhibition of the cell migration involved in the invasion process represents a potential therapeutic approach to the treatment of tumor metastasis; therefore, a novel series of derivatives of moverastins (moverastins A and B), an inhibitor of tumor cell migration, was designed and chemically synthesized. Among these moverastin derivatives, several compounds showed stronger cell migration inhibitory activity than parental moverastins, and UTKO1 was found to have the most potent inhibitory activity against the migration of human esophageal tumor EC17 cells in a chemotaxis cell chamber assay. Interestingly, although moverastins are considered to inhibit tumor cell migration by inhibiting farnesyltransferase (FTase), UTKO1 did not inhibit FTase, indicating that UTKO1 inhibited tumor cell migration by a mechanism other than the inhibition of FTase.

Despite significant advances in understanding the fundamental aspects of cancer, the development of metastatic lesions remains the predominant cause of death for most cancer patients.[1,2] Cell migration is a crucial event in the spread of cancer and, consequently, the metastatic process.[3,4] This prompted us to develop inhibitors of tumor cell migration as novel anti-metastatic drugs.

Previously, we screened for inhibitors of cancer cell migration derived from microbial origin, and obtained moverastin A and B (**1** and **2**, respectively), new members of the cylindrol family, from *Aspergillus* sp. F7720.[5] Their structures including the absolute stereochemistries were confirmed unambiguously by the synthesis as outlined in Scheme 1. Furthermore, moverastin A and B were found to inhibit FTase; therefore, moverastins were considered to inhibit the migration of tumor cells by inhibiting the farnesylation of H-Ras, and subsequent H-Ras-dependent activation of the PI3K/Akt pathway. However, because the inhibitory activity of moverastins for tumor cell migration was rather modest (IC_{50} value of 7 μM), we considered it an attractive lead compound in the search for other, more potent agents.

In this study, we chemically synthesized a series of moverastin derivatives and assessed their potential as tumor cell migration inhibitors in several in vitro assays.

Structures of moverastin derivatives (UTKO1–12) synthesized in this study are shown in Figure 1. UTKO1–6 were synthesized by employing the same approach as that for our previous synthesis of moverastins.[5] The enol triflates (**7**, **10**, **12**, **15**, **18**) were prepared starting from readily available ketones or aldehydes (**5**, **9**, **11**, **13**, **16**, respectively) as shown in Scheme 2. Coupling reactions between the enol triflates (or 2-iodopropene for UTKO4) and aldehyde **4** were carried out successfully using the Nozaki–Hiyama–Kishi procedure[6,7] and UTKO1–6 were obtained after acid hydrolysis of MOM ether. The dihydro analog (UTKO7) and etherified analogs (UTKO9 and 10) of UTKO1 were also synthesized by its hydrogenation, Mitsunobu reaction or methylation (Scheme 3). The unsaturated ketone analog of UTKO1 was also obtained by the PDC oxidation-deprotection of **19** which is the intermediate from **7** to UTKO1. UTKO11 and 12, deformylated analogs of moverastin and UTKO1, respectively, were also synthesized from aldehyde **21** instead of **4** (Scheme 4). Detailed synthetic procedure for UTKO compounds will be published elsewhere.

Next, the cell migration inhibitory activity of these moverastin derivatives was examined by the chemotaxis cell chamber (BD Biosciences) assay using conditioned medium of human esophageal tumor EC17 cells as a source of chemoattractants as previously reported with some modifications.[8] In this assay, EC17-conditioned medium was initially placed in the lower compartment. EC17 cells were incubated in the upper chamber, where they were allowed to migrate and penetrate the filter separating the chambers in order to enter the lower chamber. After 24 h of incubation, the number of cells attached to the lower side of the filter was counted. The IC_{50} values obtained in this study are listed in Table 1. Among

* Corresponding authors. Tel./fax: +81 45 566 1557 (M.I.); tel.: +81 3 5841 5119; fax: +81 3 5841 8019 (H.W.).
E-mail addresses: ashuten@mail.ecc.u-tokyo.ac.jp (H. Watanabe), imoto@bio.keio.ac.jp (M. Imoto).
† These authors contributed equally to the study.

0960-894X/$ - see front matter © 2011 Elsevier Ltd. All rights reserved.
doi:10.1016/j.bmcl.2011.01.028

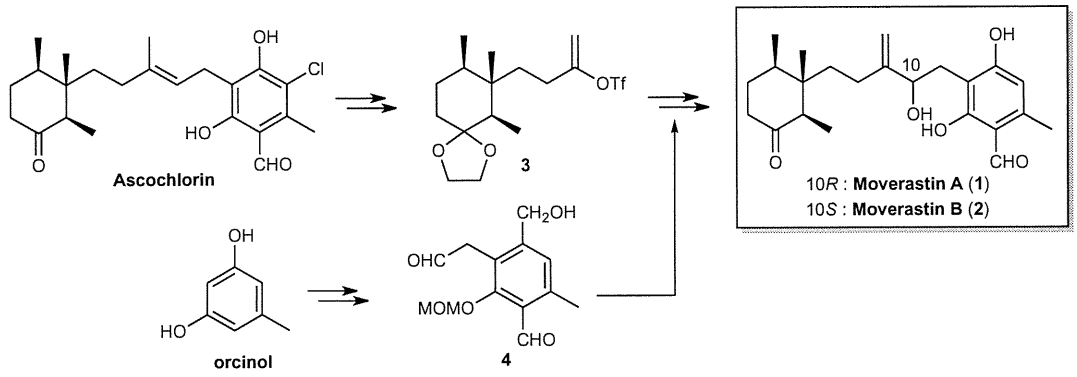

Scheme 1. Synthesis and structures of moverastin A and B.

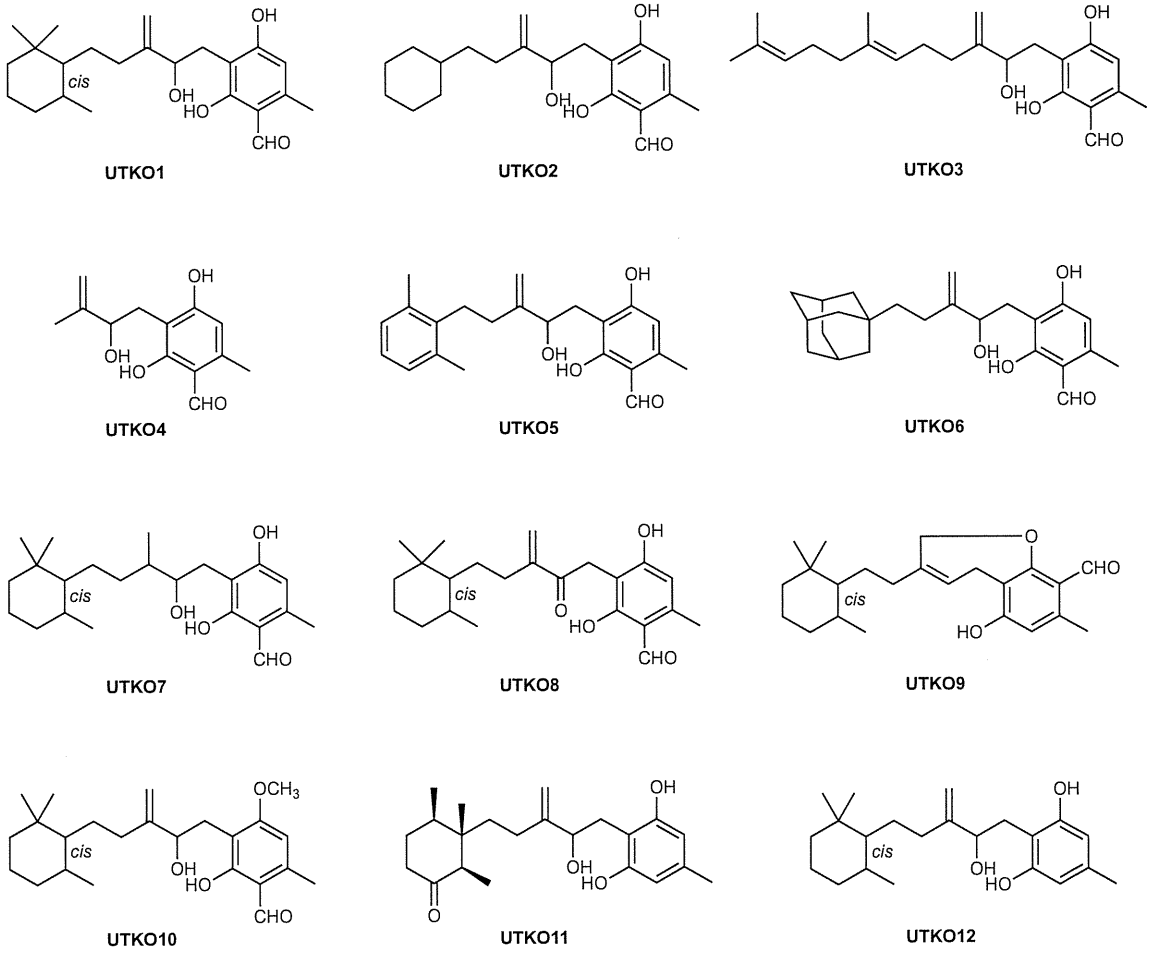

Figure 1. Structures of moverastin derivatives.

moverastin derivatives, UTKO1 showed the most potent inhibitory activity of EC17 cell migration with an IC_{50} of 1.98 μM (Fig. 2). UTKO7, UTKO9 and UTKO12 are also significantly more active inhibitors of EC17 cell migration than the parental natural product, moverastin A, with IC_{50} values of 2.12, 2.00 and 2.17 μM, respectively (Table 1). These inhibitory effects are not due to the toxic effect of the drug because their 50% inhibitory concentration for EC17 cell viability, as estimated by trypan blue dye exclusion assay, was at least five-fold higher than that for cell migration.

Previously, we found that moverastin A showed inhibitory activity against FTase, and demonstrated that moverastin A inhibited the migration of tumor cells by inhibiting the farnesylation of H-Ras;[5] therefore, next we examined the effect of moverastin derivatives on FTase in vitro. For this assay, FTase was partially purified from EC17 cells and recombinant GST-H-Ras and [^{3}H]-farnesylpyrophosphate were used as the substrates as described before.[5] As shown in Table 1, all moverastin derivatives tested, including UTKO1, UTKO7, UTKO9, and UTKO12, which showed strong inhibition of cell migration, did not inhibit FTase in vitro up to 100 μM. These results indicated that a mechanism other than the inhibition of FTase is responsible for UTKO-induced inhibition of EC17 cell migration. To examine this possibility, several cancer

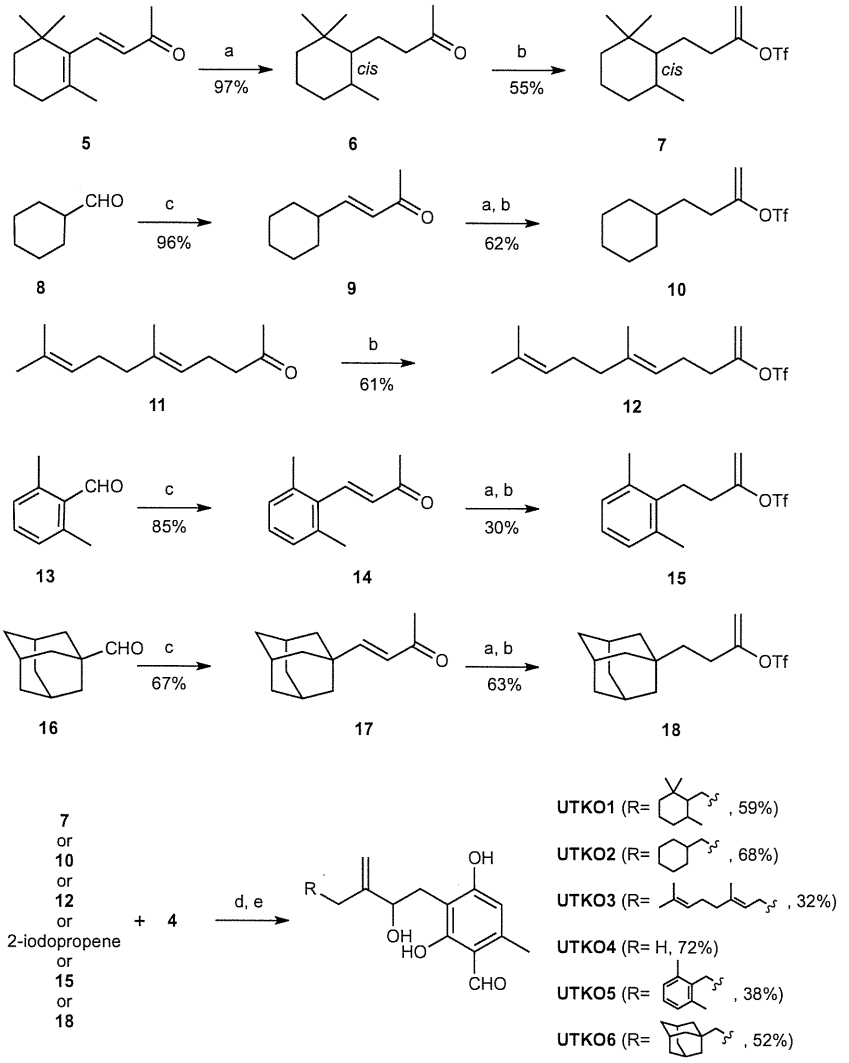

Scheme 2. Synthesis of UTKO1–6. Reagents and conditions: (a) H_2, Pd-C, EtOAc (for **6**) or EtOH (for **10**, **15** and **18**); (b) KHMDS, Comin's reagent, THF, −78 °C; (c) Ph_3P=CHCOMe, CH_2Cl_2 (for **9** and **14**) or xylene (for **17**), reflux; (d) $CrCl_2$, $NiCl_2$, DMF, rt; (e) concd HCl, THF, rt.

cell lines were investigated with respect to the inhibitory potential of moverastin A and the most potent moverastin derivative, UTKO1. The inhibitory effect of moverastin A depends on cell type, and there is a significant negative correlation between the sensitivity of each cell to moverastin A and the expression level of H-Ras, a substrate of FTase ($r = -0.86$, $p = 0.0013$) (Fig. 3). This result

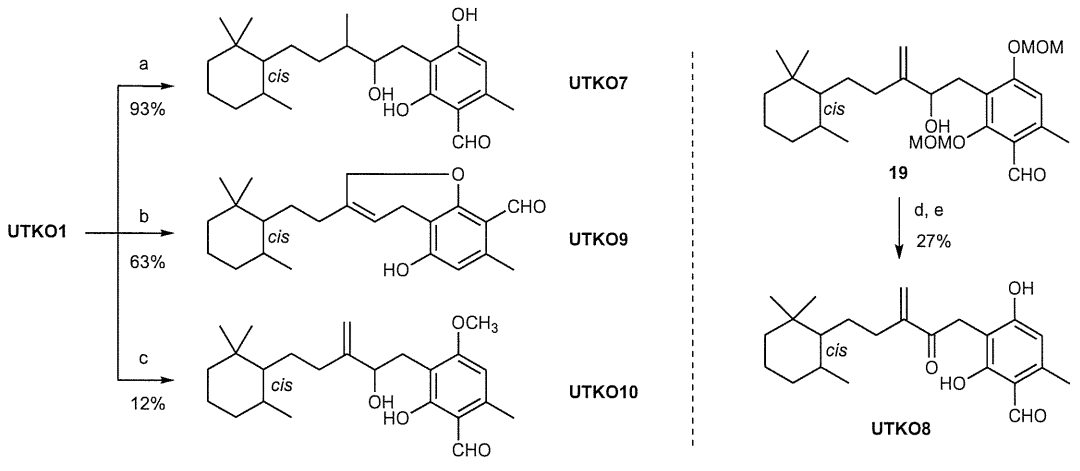

Scheme 3. Synthesis of UTKO7–10. Reagents and conditions: (a) Rh-Al_2O_3, EtOH; (b) DEAD, PPh_3, THF; (c) MeI, K_2CO_3, (*n*-Bu)$_4$N·HSO_4, EtOAc–toluene, reflux; (d) PDC, CH_2Cl_2; (e) concd HCl, THF, rt.

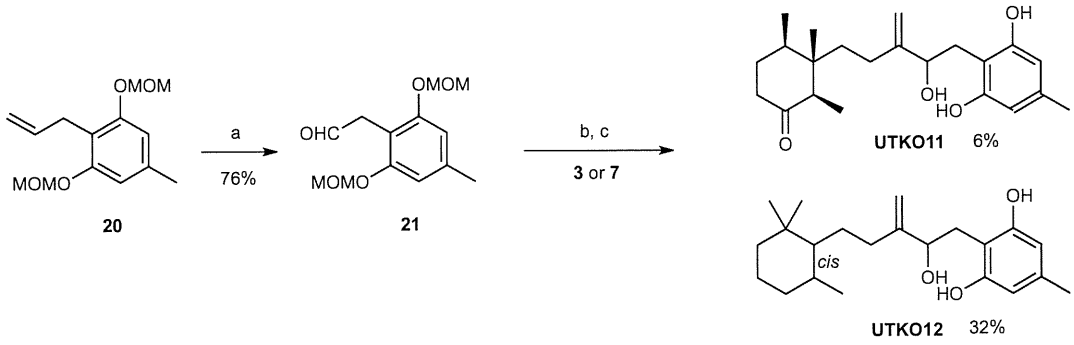

Scheme 4. Synthesis of UTKO11 and UTKO12. (a) O_3, CH_2Cl_2, −78%, then PPh_3; (b) $CrCl_2$, $NiCl_2$, DMF, rt; (c) concd HCl, THF, rt.

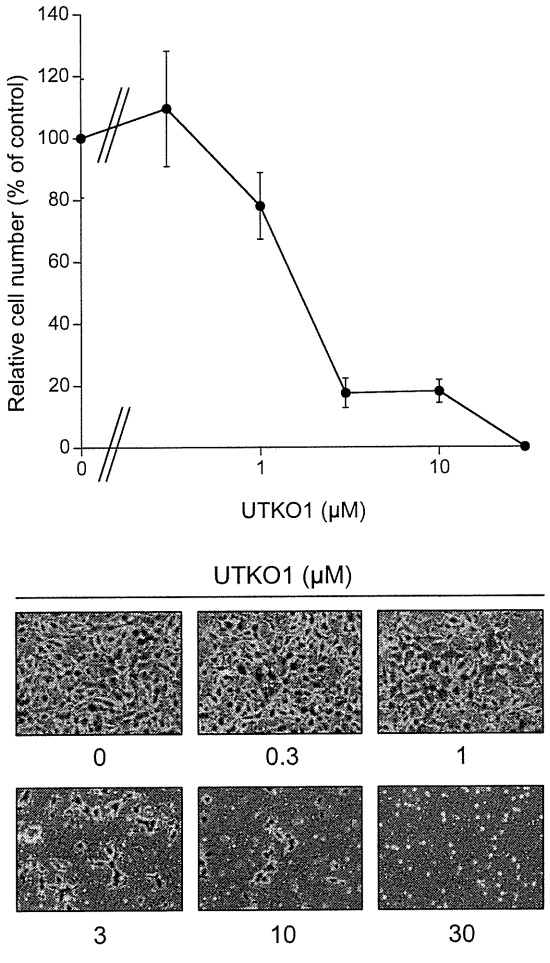

Figure 2. Effect of UTKO1 on migration of EC17 cells. EC17 cells were incubated with various concentrations of UTKO1 in the top chamber; the lower chamber contained EC17-conditioned medium, obtained from 24-hour cultures of EC17 cells maintained in RPMI1640 supplemented with 1% FBS. After 24 h, the number of cells that migrated through the filter to the lower surface was counted. The results are the mean ± SD of five different fields.

supported our previous conclusion that moverastins inhibited tumor cell migration due to the inhibition of FTase. On the other hand, the cell migration inhibitory activity of UTKO1 also depends on cell type, but there is no correlation with the expression levels of H-Ras ($r = -0.38$, $p = 0.40$) (Fig. 3). These results suggested that the inhibitory mechanism of cell migration by UTKO1 is different from that of moverastin A. To understand the molecular basis by which UTKO1 inhibits tumor cell migration, biochemical identification of the protein target for UTKO1 is now under investigation.

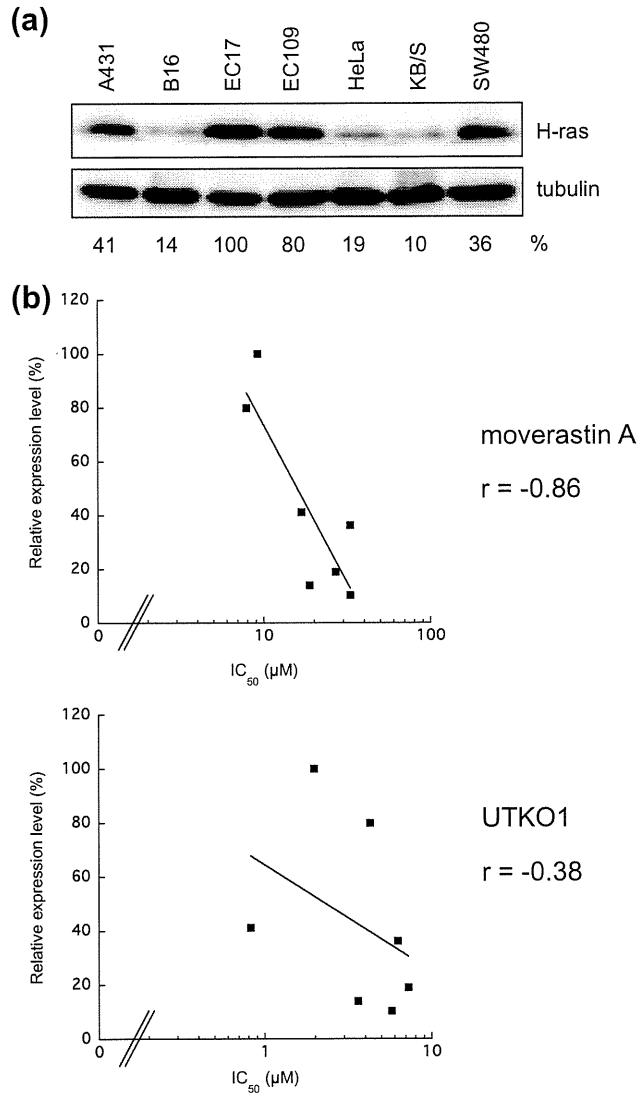

Figure 3. Correlation between expression levels of H-Ras and inhibition of migration by moverastin A and UTKO1. (a) Western blot analysis of H-Ras expression levels in seven tumor cell lines. Cell lysates were separated by SDS–PAGE and then subjected to immunoblotting using anti-H-Ras antibody. Quantitation of expression levels of H-Ras was analyzed by Image gauge and normalized with the level of tubulin. Percentages represent the relative expression level of H-Ras in tumor cells compared to the level in EC17 cells. (b) Simple linear correlations between two parameters were calculated. Correlation coefficients (r) are shown in this figure.

Table 1
Effects of UTKO compounds on cell migration, cell viability and in vitro FTase activity in EC17 cells

	IC_{50} (μM)		
	Cell migration	Cell viability[a]	FTase[b]
Moverastin A	7.22	>77	14.7
UTKO1	1.98	46	>100
UTKO2	8.43	87	>100
UTKO3	7.53	>80	>100
UTKO4	30.0	>130	>100
UTKO5	10.6	45	>100
UTKO6	6.52	55	>100
UTKO7	2.12	16	>100
UTKO8	4.41	18	>100
UTKO9	2.00	18	>100
UTKO10	4.57	18	>100
UTKO11	21.4	>28	>100
UTKO12	2.17	17	>100

[a] For cell viability assay, a trypan blue dye (15250-061, Gibco, Invitrogen) exclusion assay were used to examine cell viability and performed according to previously reported protocols.[9]

[b] For in vitro FTase assay, partially purified enzymes from EC17 cells were incubated with [^{3}H]-FPP plus recombinant GST-H-Ras in the presence or absence of test compound. The reaction was terminated by the addition of TCA. The radioactivity of the TCA insoluble fraction was measured.

Our preliminary structure–activity relationship study revealed that UTKO12 retained the same level of inhibitory activity toward EC17 cell migration as that of UTKO1, indicating that formyl group on benzene ring is not required for the inhibitory activity toward EC17 cell migration. On the other hand, the formyl groups of moverastins are essential for the FTase inhibition, because the inhibitory activity of UTKO11 toward FTase has been lost.

Although UTKO1 was initially synthesized as an analogous compound of moverastins, it possesses a different biological function from cylindrol family, and therefore, UTKO1 is expected to be a new lead compound in the search for more potent anti-metastatic and anti-cancer agents.

Acknowledgement

This work was supported by a grant from the Ministry of Education, Culture, Sports, Science, and Technology.

Supplementary data

Supplementary data associated with this article can be found, in the online version, at doi:10.1016/j.bmcl.2011.01.028. These data include MOL files and InChiKeys of the most important compounds described in this article.

References and notes

1. Gupta, P. B.; Mani, S.; Yang, J.; Hartwell, K.; Weinberg, R. A. *Cold Spring Harb. Symp. Quant. Biol.* **2005**, *70*, 291.
2. Gupta, G. P.; Massague, J. *Cell* **2006**, *127*, 679.
3. Chambers, A.; Groom, A.; MacDonald, I. *Nat. Rev. Cancer* **2002**, *2*, 563.
4. Friedl, P.; Wolf, K. *Nat. Rev. Cancer* **2003**, *3*, 362.
5. Takemoto, Y.; Watanabe, H.; Uchida, K.; Matsumura, K.; Nakae, K.; Tashiro, E.; Shindo, K.; Kitahara, T.; Imoto, M. *Chem. Biol.* **2005**, *12*, 1337.
6. Takai, K.; Kimura, K.; Kuroda, T.; Hiyama, T.; Nozaki, H. *Tetrahedron Lett.* **1983**, *24*, 5281.
7. Takai, K.; Tagashira, M.; Kuroda, T.; Oshima, K.; Utimoto, K.; Nozaki, H. *J. Am. Chem. Soc.* **1986**, *108*, 6048.
8. Saiki, I.; Murata, J.; Yoneda, J.; Kobayashi, H.; Azuma, I. *Int. J. Cancer* **1994**, *56*, 867.
9. Ormerod, M. G.; Collins, M. K.; Rodriguez-Tarduchy, G.; Robertson, D. *J. Immunol. Methods* **1992**, *153*, 57.

Biosci. Biotechnol. Biochem., **75** (2), 284–288, 2011

Quinotrierixin Inhibited ER Stress-Induced XBP1 mRNA Splicing through Inhibition of Protein Synthesis

Kohta YAMAMOTO,† Etsu TASHIRO, and Masaya IMOTO

Department of Biosciences and Informatics, Faculty of Science and Technology, Keio University, 3-14-1 Hiyoshi, Kohoku-ku, Yokohama 223-8522, Japan

Received August 25, 2010; Accepted November 22, 2010; Online Publication, February 7, 2011
[doi:10.1271/bbb.100622]

Quinotrierixin was isolated from microbes as an inhibitor of ER stress-induced XBP1 mRNA splicing, but its mode of action was unclear. We found that quinotrierixin is an inhibitor of protein synthesis, and that the required dose range of quinotrierixin to inhibit ER stress-induced XBP1 mRNA splicing was similar to that to inhibit protein synthesis. Furthermore, we also found that quinotrierixin inhibited the ER stress-induced increases of unfolded protein response-related genes such as GRP78, CHOP, EDEM, ERdj4, and p58^{IPK}. Thus, we showed that quinotrierixin inhibited the ER stress-induced unfolded protein response, possibly due to its inhibitory activity of protein synthesis.

Key words: quinotrierixin; ER stress; XBP1; protein synthesis inhibitor

Newly synthesized polypeptides that are secreted or localized in the plasma membrane are post- or co-translationally translocated into the lumen of the endoplasmic reticulum (ER), where they are modified, folded, and assembled correctly prior to transport to the Golgi apparatus. However, when cells are faced with cytotoxic conditions, such as hypoxia and nutrient deprivation, these folding reactions are compromised and protein aggregation occurs. The unfolded proteins are retained in the ER, and the accumulation of unfolded proteins causes ER stress.[1] As a consequence, the cell activates adaptive signaling pathways that are programmed to enhance folding capabilities and to limit the folding load on the ER. This response is called the unfolded protein response (UPR).

In mammalian cells, UPR is regulated in part by ER membrane-localized IRE1α.[2–4] IRE1α induces unconventional X-box binding protein 1 (XBP1) mRNA splicing. Twenty-six nts of XBP1 mRNA are spliced out to lead the shift in the open reading frame. Translation of spliced XBP1 mRNA produces a potent transcription factor called XBP1s (the "s" indicates spliced).[5,6] XBP1s upregulates gene expression that enhances ER protein folding capacity and quality control.[7] Furthermore, it has been reported that there is a link between XBP1 and human disease, including solid tumor and inflammatory bowel disease.[8–14] Therefore, small molecule inhibitors of ER stress-induced XBP1 mRNA splicing would be very useful in fundamental research into UPR signaling, and might eventually find clinical application.

In a previous study, we established a screening system to identify small molecule inhibitors of XBP1 mRNA splicing. We have also reported that novel trieneansamycin group compounds, quinotrierixin and trierixin, inhibited ER stress-induced XBP1 mRNA splicing in HeLa cells.[15–18] In this study, we found that quinotrierixin inhibited protein synthesis. Moreover, we investigated the relationship between quinotrierixin-inhibited ER stress-induced XBP1 mRNA splicing and protein synthesis.

Materials and Methods

Materials. Quinotrierixin, trierixin, and trienomycin A were prepared as described in our previous reports.[15,17] Cytotrienin A was kindly provided by Dr. H. Osada (RIKEN, Japan). Cycloheximide, anisomycin, and puromycin were purchased from Sigma (St. Louis, MO).

Cell culture. Human epithelial adenocarcinoma cell line HeLa was cultured in DMEM supplemented with 8% FBS.

RT-PCR analysis (XBP1 mRNA splicing assay). As reported previously,[15] HeLa cells were seeded in 12-well plates at 5×10^4 cells/well, and then incubated with 10 μg/mL of tunicamycin with and without quinotrierixin and other protein synthesis inhibitors for 4 h. Subsequently, total RNA was extracted from the HeLa cells using TRIzol reagent (Invitrogen, Carlsbad, CA). Aliquots of 2.0 μg of the total RNA were treated with M-MLV reverse transcriptase (Promega, Madison, WI) to produce first-strand cDNA, which was subjected to polymerase chain reaction (PCR) with KOD plus polymerase (Toyobo, Osaka, Japan) using a pair of primers corresponding to nucleotides 505–524 and 609–629 of XBP1 cDNA. The amplified products were separated by electrophoresis on a 8% polyacrylamide gel and visualized by ethidium bromide staining.

Real-time RT-PCR. Real-time reverse transcription (RT)–polymerase chain reaction (PCR) was performed using SYBR Premix Ex Taq (Takara, Siga, Japan). The primer set was as follows: for GRP78, forward 5′-GCTCGACTCGAATTCCAAAG-3′ and reverse 5′-GATCACCAGAGAGCACACCA-3′; for CHOP, forward 5′-GCGCATGAAGGAGAAAGAAC-3′ and reverse 5′-TCACCATTCGGTCAATCAGA-3′; for ERdj4, forward 5′-AAAATAAGAGCCCGGATGCT-3′ and reverse 5′-CGCTTCTTGGATCCAGTGTT-3′; for EDEM, forward 5′-TGGACTGCAGGTGCTGATAG-3′ and reverse 5′-GGATTCTTGGTTGCCTGGTA-3′; for P58^{IPK}, forward 5′-CTCAGTTTCATGCTGCCGTA-3′ and reverse 5′-TTGCTGCAGTGAAGTCCATC-3′; and for GAPDH, forward 5′-AGGTCGGAGTCAACGGATTT-3′ and reverse 5′-TAGTTGAGGTCAATGAAGGG-3′.

Measurement of macromolecular synthesis. HeLa cells were seeded in 24-well plates at 5×10^4 cells/well and cultured overnight. Each culture well was refilled with fresh Dulbecco's Modified Eagle's

† To whom correspondence should be addressed. Tel: +81-45-566-1793; Fax: +81-45-566-1557; E-mail: tashiro@bio.keio.ac.jp

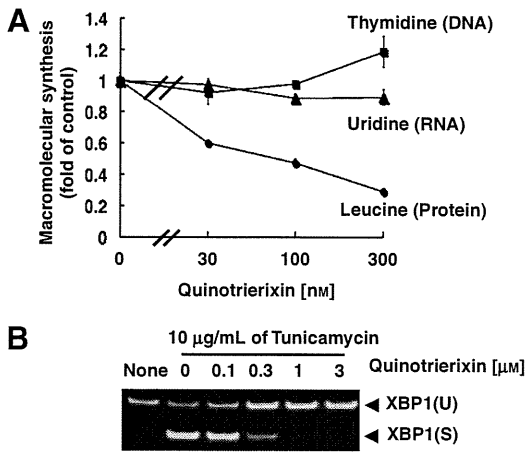

Fig. 1. Quinotrierixin, Cycloheximide, and Anisomycin Inhibited ER Stress-Induced XBP1 mRNA Splicing and Protein Synthesis.

A, Quinotrierixin inhibited protein synthesis in HeLa cells. HeLa cells were treated with the indicated concentrations of qunotrierixin with [^{3}H]-leucine, [^{3}H]-thymidine, or [^{3}H]-uridine for 1 h. The radioactivity of the macromolecular fraction was measured with a liquid scintillation counter. The representative data are the means for three independent studies. B, Quinotrierixin inhibited tunicamycin-induced XBP1 mRNA splicing. HeLa cells were treated with 10 μg/mL of tunicamycin with and without the indicated concentrations of quinotrierixin for 4 h. The cells were collected and extracted RNA was subjected to RT-PCR. Spliced and unspliced XBP1 mRNA was detected as described in "Materials and Methods." XBP1(U) and XBP1(S) indicate unspliced and spliced XBP1 mRNA respectively.

Medium (DMEM) containing 0.2% fetal bovine serum (FBS). For measurement of protein synthesis, cells were treated with 2 μCi [^{3}H]-leucine, 0.5 μCi [^{3}H]-thymidine or 0.5 μCi [^{3}H]-uridine, radioactive protein, and DNA or RNA synthesis precursor, with and without the indicated compounds for 1 h at 37 °C. After incubation, the medium was removed and the macromolecular fraction was fixed with ice-cold 10% trichloroacetic acid (TCA). Each well was washed with ice-cold 10% TCA twice, and 0.5 N NaOH was added. Radioactivity was measured with a liquid scintillation counter.

Data analysis. For determination of IC_{50} values against tunicamycin-induced XBP1 mRNA splicing, the spliced-XBP1 mRNA bands visualized with ethidium bromide staining were quantified by densitometry. IC_{50} values were determined from the dose-response curves of the inhibition of XBP1 mRNA splicing activity, where the intensity of spliced-XBP1 mRNA bands of tunicamycin treatment was defined as 100%.

IC_{50} values against protein synthesis were determined from dose-response curves, the radioactivity of non-treatment control was defined as 100%.

Real-time RT-PCR data were analyzed by paired *t*-tests to evaluate differences in means among three independent experiments, $^*p < 0.05$ and $^{**}p < 0.01$.

Results

Quinotrierixin inhibited XBP1 mRNA splicing and protein synthesis

Quinotrierixin was identified as an inhibitor of ER stress-induced XBP1 mRNA splicing, but its mode of action was unclear. Previously, cycloheximide, a well-known protein synthesis inhibitor, was reported to inhibit ER stress-induced XBP1 mRNA splicing.[19] Hence, we examined whether quinotrierixin would inhibit protein synthesis. As shown in Fig. 1A, quinotrierixin inhibited [^{3}H]-leucine uptake into the macromolecular fraction of HeLa cells in a dose-dependent manner. On the other hand, neither [^{3}H]-thymidine uptake nor [^{3}H]-uridine uptake was inhibited by quinotrierixin at up to 300 nm. These results indicate that quinotrierixin inhibits protein synthesis without affecting DNA or RNA synthesis (Fig. 1A). Because the dose range of quinotrierixin for inhibiting protein synthesis was similar to that for inhibiting tunicamycin and 2-deoxyglucose (2DG), both of which are known as ER stress inducers, -induced XBP1 mRNA splicing (Fig. 1B and Supplemental Fig. 1; see *Biosci. Biotechnol. Biochem.* Web site), another three triene-ansamycin group compounds, which inhibited ER stress-induced XBP1 mRNA splicing, were assessed for their ability to inhibit protein synthesis. As shown in Table 1, trierixin, trienomycin A, and cytotrienin A inhibited protein synthesis at almost the same concentration as for the inhibition of tunicamycin-induced XBP1 mRNA splicing.

Table 1. Inhibitory Activities of Triene-Ansamycin Group Compounds, Cycloheximide, Anisomycin, and Puromycin against ER Stress-Induced XBP1 Activation and Protein Synthesis

	XBP1 inhibition IC_{50} value [nM]	Protein synthesis inhibition IC_{50} value [nM]
Quinotrierixin	85	120
Trierixin	17	55
Trienomycin A	47	38
Cytotrienin A	190	160
Cycloheximide	530	680
Anisomycin	240	120
Puromycin	>20,000	4,400

Quinotrierixin inhibited unfolded protein response

Next, to determine whether quinotrierixin would affect other ER stress-induced unfolded protein responses, we evaluated the effects of quinotrierixin on the mRNA levels of UPR related genes, GRP78, CHOP, EDEM, ERdj4, and p58^{IPK}, under ER stress conditions. We found that quinotrierixin completely suppressed the increases in GRP78, CHOP, EDEM, ERdj4, and p58^{IPK} mRNA induced by tunicamycin or 2DG at the same concentration as for inhibition of protein synthesis and XBP1 mRNA splicing. (Fig. 2 and Supplemental Fig. 2). These results indicate that quinotrierixin did not specifically inhibit ER stress-induced XBP1 mRNA splicing, but rather that quinotrierixin would induce the shutdown of all ER stress-induced UPR.

Cycloheximide and anisomycin, but not puromycin, inhibited the unfolded protein response

To confirm that protein synthesis inhibition due to quinotrierixin results in the suppression of ER stress-induced UPR, we determined whether other protein synthesis inhibitors would inhibit ER stress-induced UPR. As shown in Figs. 3A and 4 and Supplemental Figs. 1 and 2, anisomycin as well as cycloheximide inhibited not only XBP1 mRNA splicing but also the UPR gene upregulation induced by tunicamycin and by 2DG. On the other hand, puromycin failed to inhibit the XBP1 mRNA splicing induced by tunicamycin and by 2DG under conditions in which puromycin inhibited protein synthesis, as judged by [^{3}H]-leucine uptake into the macromolecular fraction of the HeLa cells (Table 1,

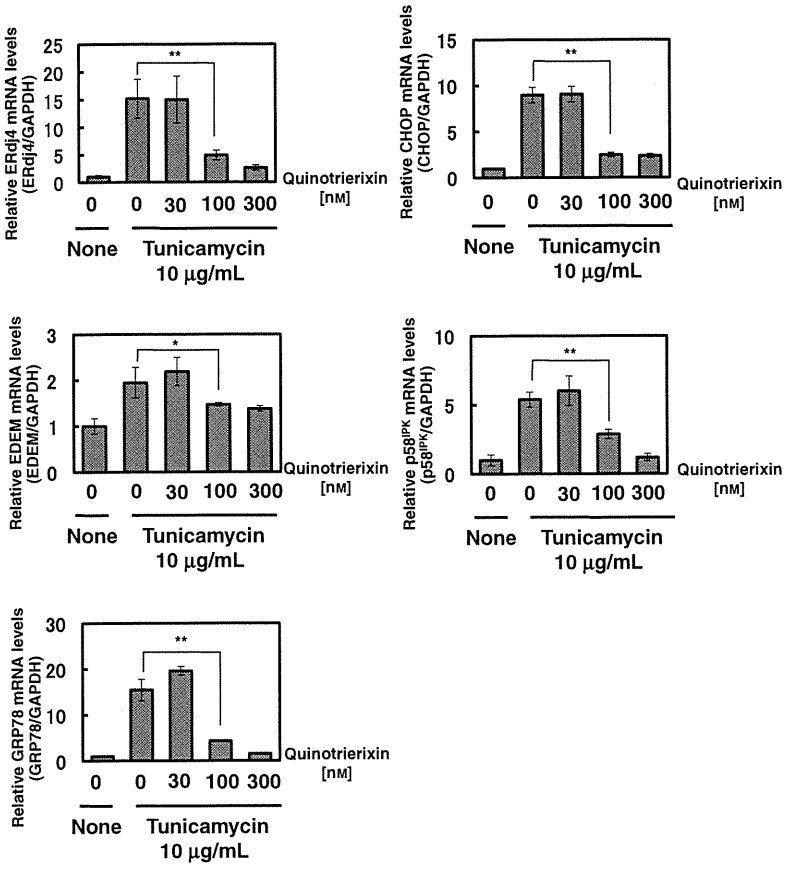

Fig. 2. Quinotrierixin Inhibited the Unfolded Protein Response.

Quinotrierixin suppressed tunicamycin-increased ERdj4, EDEM, GRP78, CHOP, and $p58^{IPK}$ mRNA. HeLa cells were treated with 10 μg/mL of tunicamycin with and without the indicated concentrations of quinotrierixin for 8 h. The cells were collected and RNA was extracted. ERdj4, EDEM, GRP78, CHOP, and $p58^{IPK}$ mRNA levels were evaluated by real-time RT-PCR. Each mRNA was normalized with the mRNA levels of GAPDH. Data are the means ± SD among three independent experiments, $^{*}p < 0.05$ and $^{**}p < 0.01$.

Fig. 3A, and Supplemental Fig. 3). Rather, consistently with a previous report,[20] single treatment of cells with puromycin induced XBP1 mRNA splicing (Fig. 3B). Both spliced and unspliced XBP1 mRNA were weakly reduced when the cells were treated with puromycin together with tunicamycin, but this was probably due to cytotoxicity, because puromycin induced cell membrane disruption at 6 μM after 4 h of treatment with puromycin together with tunicamycin (data not shown).

Discussion

In this study, we found for the first time that triene-ansamycin group compounds, including quinotrierixin, inhibited protein synthesis. Although several biological activities of triene-ansamycin antibiotics have been reported, the activity of protein synthesis inhibition has not been reported. This finding raises the possibility that some biological activities of triene-ansamycin group compounds, such as apoptosis induction,[21] inhibition of NO production,[22] and inhibition of osteoblastic resorption,[23] can be explained by inhibitory activity of protein synthesis.

Quinotrierixin and other protein synthesis inhibitors suppressed not only ER stress-induced XBP1 mRNA splicing but also other UPR, such as transcription of the UPR genes GRP78, CHOP, EDEM, ERdj4, and $p58^{IPK}$, at the same concentration as for inhibition of protein synthesis. The only exception was puromycin, which did

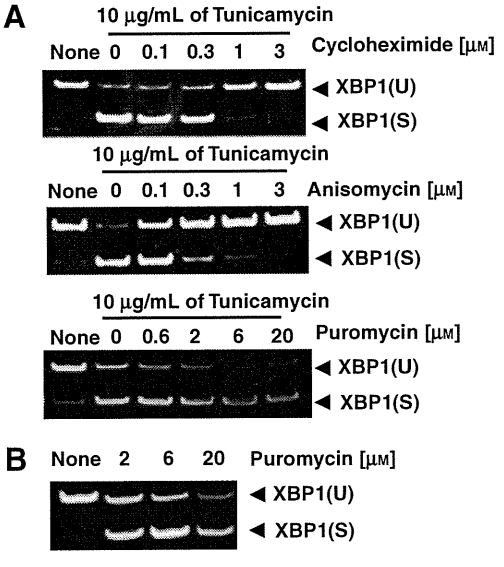

Fig. 3. Cycloheximide and Anisomycin, but Not Puromycin, Inhibited XBP1 mRNA Splicing.

A, Cycloheximide and anisomycin but not puromycin inhibited tunicamycin-induced XBP1 mRNA splicing. HeLa cells were treated with 10 μg/mL of tunicamycin with and without the indicated concentrations of cycloheximide, anisomycin, or puromycin for 4 h. B, Puromycin induced XBP1 mRNA splicing. HeLa cells were treated with the indicated concentrations of puromycin for 4 h. The cells were collected, and extracted RNA was subjected to RT-PCR. Spliced and unspliced XBP1 mRNA was detected as described in "Materials and Methods." XBP1(U) and XBP1(S) indicate unspliced and spliced XBP1 mRNA respectively.

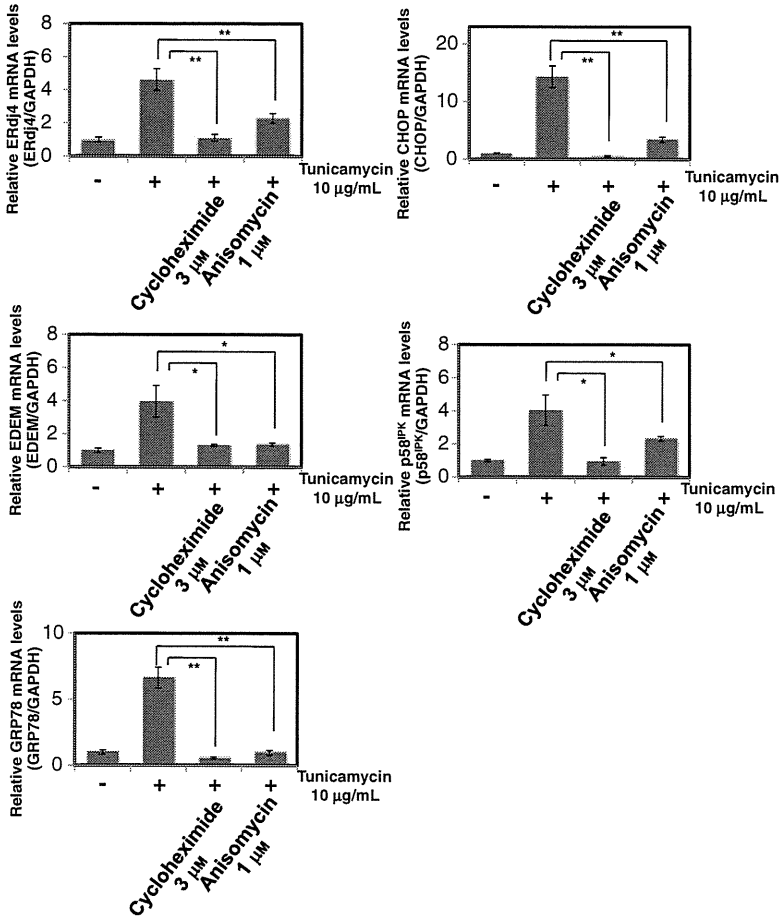

Fig. 4. Cycloheximide and Anisomycin Inhibited the Unfolded Protein Response.

Cycloheximide and anisomycin suppressed tunicamycin-increased ERdj4, EDEM, GRP78, CHOP, and $p58^{IPK}$ mRNA. HeLa cells were treated with 10 μg/mL of tunicamycin with and without the indicated concentrations of cycloheximide or anisomycin for 8 h. Cells were collected and RNA was extracted. ERdj4, EDEM, GRP78, CHOP, and $p58^{IPK}$ mRNA levels were evaluated by real-time RT-PCR. Each mRNA was normalized with the mRNA levels of GAPDH. Data are the means ± SD among three independent experiments, $^{*}p < 0.05$ and $^{**}p < 0.01$.

not inhibit ER stress-induced XBP1 mRNA splicing. As previously reported, puromycin alone induced UPR in HeLa cells. Hence a different effect on UPR by protein synthesis inhibitor appears to be dependent on the inhibitory mechanism of the protein synthesis inhibitor. Puromycin has been reported to enforce nascent polypeptides to release from the ribosome halfway through the elongation reaction.[24] Thus, un-maturated proteins might influx into the ER and accumulate, and then induce ER stress as unfolded proteins. In contrast, cycloheximide and anisomycin inhibited polypeptide release from the ribosomes due to inhibition of ribosome translocation and to inhibition of peptidyl transfer respectively.[25] This indicates that un-maturated proteins produced by cycloheximide or anisomycin cannot move to the ER, and fail to induce ER stress. This inhibitory mechanism of cycloheximide and anisomycin may explain why they suppress ER stress-induced UPR. These compounds prevent further influx of newly synthesized proteins into the ER, which results in a reduction in ER stress.

At present, the inhibitory mechanism in protein synthesis due to quinotrierixin remains unclear. However, because quinotrierixin suppressed ER stress-induced UPR as did cycloheximide and anisomycin but not puromycin, the mode of action of quinotrierixin would be similar to cycloheximide and anisomycin. Thus, it is likely that quinotrierixin blocked polypeptide release from the ribosomes. But further study is needed to elucidate the mechanism.

Acknowledgments

We thank Dr. Hiroyuki Osada (RIKEN, Japan) for kindly providing us with cytotrienin A. This study was partly supported by grants from Takeda Science Foundation and Suzuken Memorial Foundation. This work was also supported by a Grant-in-Aid for Scientific Research from the Ministry of Education, Culture, Sports, Science, and Technology of Japan. This study was supported in part by the Global COE Program for Human Metabolomic Systems Biology of MEXT, Japan.

References

1) Ellgaard L and Helenius A, *Curr. Opin. Cell Biol.*, **13**, 431–437 (2001).
2) Zhou J, Liu CY, Back SH, Clark RL, Peisach D, Xu Z, and Kaufman RJ, *Proc. Natl. Acad. Sci. USA*, **103**, 14343–14348 (2006).
3) Wang XZ, Harding HP, Zhang Y, Jolicoeur EM, Kuroda M, and Ron D, *EMBO J.*, **17**, 5708–5717 (1998).
4) Credle JJ, Finer-Moore JS, Papa FR, Stroud RM, and Walter P, *Proc. Natl. Acad. Sci. USA*, **102**, 18773–18784 (2005).
5) Calfon M, Zeng H, Urano F, Till JH, Hubbard SR, Harding HP, Clark SG, and Ron D, *Nature*, **415**, 92–96 (2002).

6) Yoshida H, Matsui T, Yamamoto A, Okada T, and Mori K, *Cell*, **107**, 881–891 (2001).
7) Lee AH, Iwakoshi NN, and Glimcher LH, *Mol. Cell. Biol.*, **23**, 7448–7459 (2003).
8) Marciniak SJ and Ron D, *Physiol. Rev.*, **86**, 1133–1149 (2006).
9) Ozcan U, Cao Q, Yilmaz E, Lee AH, Iwakoshi NN, Ozdelen E, Tuncman G, Görgün C, Glimcher LH, and Hotamisligil GS, *Science*, **306**, 457–461 (2004).
10) Fujimoto T, Onda M, Nagai H, Nagahata T, Ogawa K, and Emi M, *Breast Cancer*, **10**, 301–306 (2003).
11) Shuda M, Kondoh N, Imazeki N, Tanaka K, Okada T, Mori K, Hada A, Arai M, Wakatsuki T, Matsubara O, Yamamoto N, and Yamamoto M, *J. Hepatol.*, **38**, 605–614 (2003).
12) Feldman DE, Chauhan V, and Koong AC, *Mol. Cancer Res.*, **3**, 597–605 (2005).
13) Romero-Ramirez L, Cao H, Nelson D, Hammond E, Lee AH, Yoshida H, Mori K, Glimcher LH, Denko NC, Giaccia AJ, Le QT, and Koong AC, *Cancer Res.*, **64**, 5943–5947 (2004).
14) Kaser A, Lee AH, Franke A, Glickman JN, Zeissig S, Tilg H, Nieuwenhuis EE, Higgins DE, Schreiber S, Glimcher LH, and Blumberg RS, *Cell*, **134**, 743–756 (2008).
15) Tashiro E, Hironiwa N, Kitagawa M, Futamura Y, Suzuki S, Nishio M, and Imoto M, *J. Antibiot.* (Tokyo), **60**, 547–553 (2007).
16) Futamura Y, Tashiro E, Hironiwa N, Kohno J, Nishio M, Shindo K, and Imoto M, *J. Antibiot.* (Tokyo), **60**, 582–585 (2007).
17) Kawamura T, Tashiro E, Yamamoto K, Shindo K, and Imoto M, *J. Antibiot.* (Tokyo), **61**, 303–311 (2008).
18) Kawamura T, Tashiro E, Shindo K, and Imoto M, *J. Antibiot.* (Tokyo), **61**, 312–317 (2008).
19) Elouil H, Bensellam M, Guiot Y, Vander Mierde D, Pascal SM, Schuit FC, and Jonas JC, *Diabetologia*, **50**, 1442–1452 (2007).
20) Croons V, Martinet W, Herman AG, and De Meyer GR, *J. Pharmacol. Exp. Ther.*, **325**, 824–832 (2008).
21) Sugita M, Natori Y, Sueda N, Furihata K, Seto H, and Otake N, *J. Antibiot.* (Tokyo), **35**, 1474–1479 (1982).
22) Kim WG, Song NK, and Yoo ID, *J. Antibiot.* (Tokyo), **55**, 204–207 (2002).
23) Feuerbach D, Waelchli R, Fehr T, and Feyen JH, *J. Biol. Chem.*, **270**, 25949–25955 (1995).
24) Azzam ME and Algranati ID, *Proc. Natl. Acad. Sci. USA*, **70**, 3866–3869 (1973).
25) Pestka S, *Annu. Rev. Microbiol.*, **25**, 487–562 (1971).

Biosci. Biotechnol. Biochem., **75** (2), 367–369, 2011

Note

A New, Convenient Cell-Based Screening Method for Small-Molecule Glycolytic Inhibitors

Mitsuhiro KITAGAWA,* Mayuko MISAWA, Seiichiro OGAWA, Etsu TASHIRO, and Masaya IMOTO†

Department of Biosciences and Informatics, Faculty of Science and Technology, Keio University, 3-14-1 Hiyoshi, Kohoku-ku, Yokohama, Kanagawa 223-8522, Japan

Received September 28, 2010; Accepted October 30, 2010; Online Publication, February 7, 2011
[doi:10.1271/bbb.100693]

To counteract active glycolysis in tumors, we developed a new, convenient cell-based screening system to identify an inhibitor of glycolysis. Using this system, we searched for an inhibitor in the synthetic Carbasugar library and found two candidates. It was found that both inhibited glycolysis by suppressing the glucose uptake step in tumor cells.

Key words: inhibitor screening; tumor glycolysis; glucose uptake inhibitor; carbasugar library

It is widely recognized that solid tumors exposed to hypoxia can survive and grow aggressively despite low oxygen and limited nutrition. Active glycolysis, well known as the Warburg effect, plays an important role as a lifeline for tumor survival and growth under these conditions by fueling cancer cells with ATP energy and supplying bioorganic components, such as nucleotides and fatty acids for growth.[1,2] Hence, glycolysis inhibitors are expected to be candidate drugs for tumor treatment, and hence screening research on these inhibitors has potential for cancer therapy. Many glycolytic inhibitors have been found to be inhibitors of key glycolytic enzymes,[3–5] but it is not easy to evaluate whether these glycolytic enzyme inhibitors actually modulate glycolysis in living cells. Hence, the establishment of a new cell-based screening system is required for the discovery of small, cell-permeable molecules that induce glycolysis inhibition in living cells.

Here we propose a novel cell-based screening method for glycolytic inhibitors.

Filopodia are spike-like cell membrane projections that contribute to tumor metastasis. Recently, we found that glycolytic suppression resulted in inhibition of filopodium protrusion in cancer cells only when their mitochondrial respiration was restricted.[6] This inhibition of filopodium protrusion might occur due to decreased intracellular ATP concentration caused by blocking of both glycolysis and mitochondrial respiration.[6–9] Since the test for filopodium inhibition is an easy, low-cost, quick assay, here we utilized it as a cell-based screening method for a new glycolytic inhibitor. In the assay, screening samples were added to human adenocarcinoma A431 cells co-treated with and without the mitochondrial respiratory inhibitor rotenone and

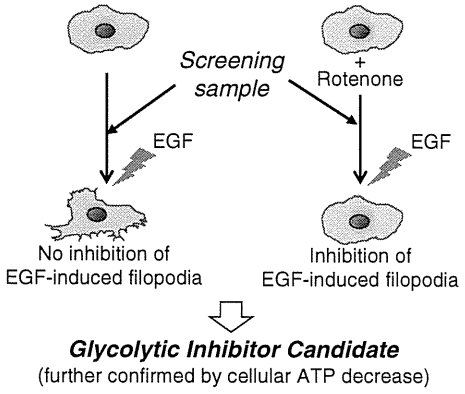

Fig. 1. Image of Screening for Glycolytic Inhibitors by EGF-Induced Filopodium Protrusion Assay.

were examined for their inhibitory effect on EGF-induced filopodium protrusion, which is easily judged by microscopic observation in 30 min (Fig. 1). A potential glycolytic inhibitor would inhibit filopodium protrusion only by co-treatment with a mitochondrial respiratory inhibitor. In the event, 2-deoxy-D-glucose (2DG), an inhibitor of glycolytic enzyme hexokinase, inhibited EGF-induced filopodium protrusion only in the presence of rotenone (Fig. 2A), indicating that this assay system works successfully. As screening source, we used a chemical library composed of 1,069 compounds, mainly cyclohexanepolyols and derivatives thereof. These compounds were carbocyclic analogs of hexopyranoses called carbasugars. The carbasugar library was originally prepared in the course of studies of the development of bioactive substances, such as antibacterial and anticancer compounds, sweeteners, and enzyme inhibitors by Ogawa *et al.* The structural features of carbasugars possibly mimic those of glucose or glycolytic metabolites, and thus are an attractive screening source for glycolytic inhibitors.

In the first screening run, 10 μg/mL of compounds (in DMSO) were tested. Hit candidates in the first run were tested again at various concentrations. We identified two compounds (sample #169 [1,4,5,6-tetra-*O*-acetyl-2-*O*-mesyl-3-*O*-benzoyl-*myo*-inositol[10]] and sample #288 [1,2,4,5-tetra-*O*-acetyl-3,6-di-*O*-tosyl-*muco*-inositol[11]]) as glycolytic inhibitors that showed filopodium inhibition only in the presence of the mitochondrial respira-

† To whom correspondence should be addressed. Fax: +81-45-566-1557; E-mail: imoto@bio.keio.ac.jp
* Present address: *Institute for Advanced Biosciences, Keio University, 246-2 Mizukami, Kakuganji, Tsuruoka, Yamagata 997-0052, Japan*
Abbreviations: EGF, epidermal growth factor; 2DG, 2-deoxy-D-glucose; RTN, rotenone

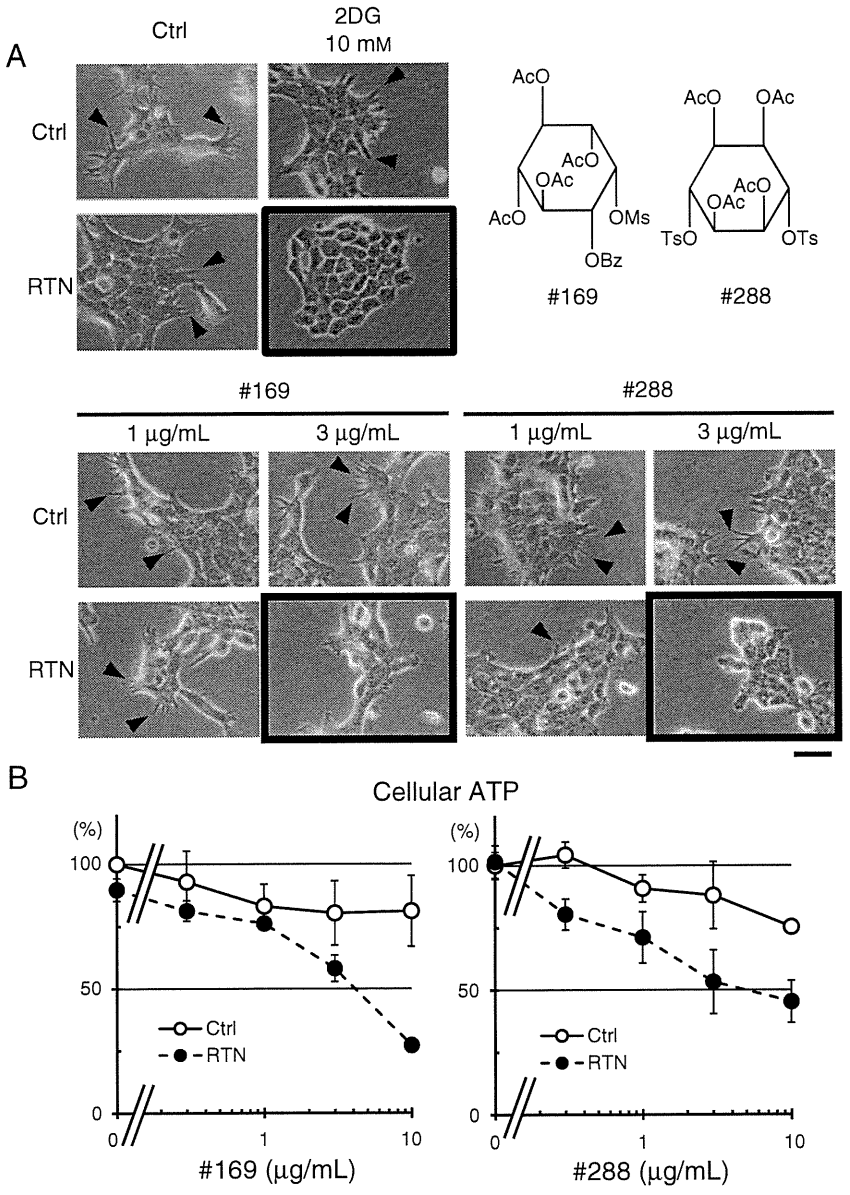

Fig. 2. Screening for Glycolytic Inhibitors in the Carbasugar Library.

A, Samples from the pseudo-sugar library were originally prepared and re-crystallized for storage by Ogawa *et al.* Two compounds, #169[10] and #288,[11] in the library, showed filopodia inhibition only in the presence of the mitochondrial respiratory inhibitor. The assay method was as described previously.[6] Hexokinase inhibitor 2-deoxyglucose (2DG, 10 mM) was used as positive control, and rotenone (RTN, 300 nM) was used to inhibit mitochondrial respiration. The arrowhead indicates filopodia, and the framed photos showed filopodium inhibition. Scale bar, 40 μm. Data represent two independent experiments. Sample purity was confirmed by LC-MS. B, Glycolytic inhibition. A431 cells were treated with the test compounds in the presence of rotenone (RTN, 300 nM) and of its solvent, ethanol, for 30 min. Cellular ATP levels were determined by luciferin-luciferase reaction (Sigma, St. Louis, MO). Bars, s.d. (n = 3). Data represent three independent experiments.

tory inhibitor rotenone (Fig. 2A). Next we tested to determine whether they would indeed suppressed glycolysis. It has been stated that glycolytic limitation caused a marked ATP decrease in tumor cells when mitochondria respiration was inhibited.[6,8] As shown in Fig. 2B, the above candidate glycolytic inhibitors slightly decreased cellular ATP in the absence of the mitochondria respiratory inhibitor. However, in combination with the mitochondria respiratory inhibitor, they did decrease intracellular ATP levels in a dose-dependent manner, indicating that they inhibited glycolysis.

To investigate further how they inhibit glycolysis, we examined their effects on the 3 steps of glycolysis: glucose uptake, hexokinase, and pyruvate kinase. It has been reported that these steps play important roles in accelerated glycolysis in tumor metabolism, and higher expression levels of the proteins facilitating these steps are frequently observed.[3,12–14] Neither #169 nor #288 affected hexokinase or pyruvate kinase reactions at up to 30 μg/mL (Fig. 3A), but they inhibited the glucose uptake step dose-dependently, with IC_{50} values of 4.5 μg/mL for #169 and 2.7 μg/mL for #288 (Fig. 3B). Inhibition of glucose uptake was similar to that due to decreasing intracellular ATP levels in the presence of rotenone, as shown in Fig. 2B, suggesting that both #169 and #288 suppressed glycolysis by inhibiting cellular glucose uptake.

In summary, here we propose a new, convenient screening assay for glycolytic inhibitors. We found two glycolytic inhibitors in a carbasugar library. They limited glycolysis by inhibiting glucose uptake at several μg/mL concentrations.

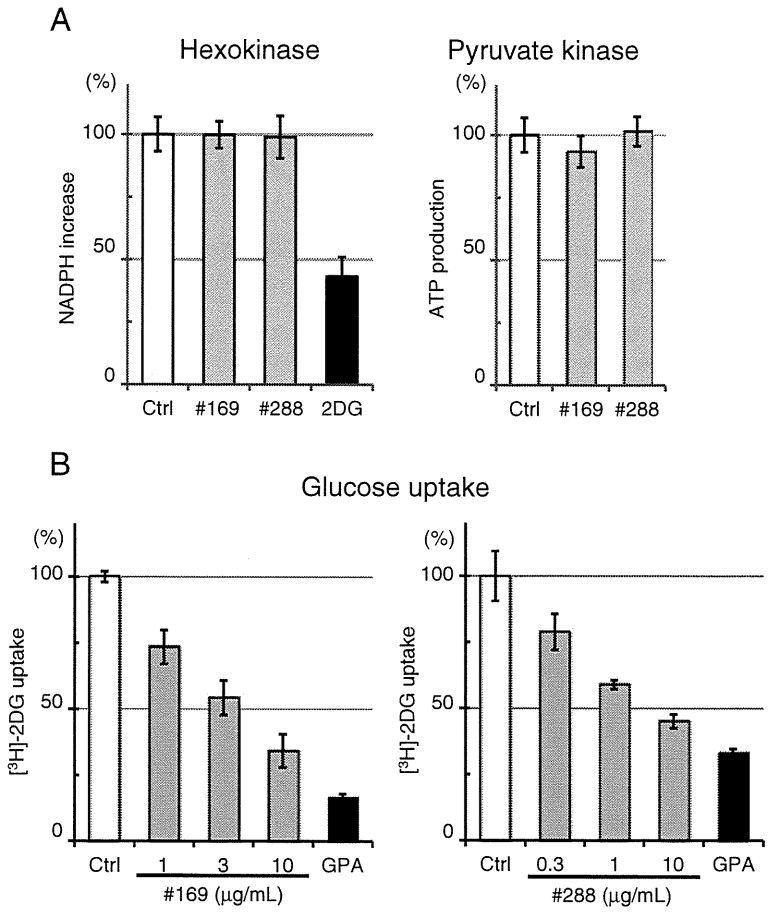

Fig. 3. Inhibition of the Glucose Uptake Step to Explain Glycolytic Suppression by #169 and #288.

A, Effects of compounds on the activities of two of the rate-limiting enzymes *in vitro*. Hexokinase activity was determined as described previously.[6] For pyruvate kinase activity, purified recombinant human pyruvate kinase 1 was used. The complete human pyruvate kinase 1 from HeLa cDNA was cloned into *E. coli* expression vector pRSETc. The reaction (3 μM ADP and 0.3 μM F1, 6P for the substrate in PK buffer, containing 5 mM $MgCl_2$, 0.1 mg/mL BSA, 2 mM DTT, 1 mM EDTA, 50 mM KCl, 50 mM Tris pH 7.7) for 30 min was quenched with TCA and neutralized. Enzymatic activity was calculated by ATP production. Bars, s.d. (n = 3). B, Inhibition of glucose uptake by #169 and #288. The assay method was as described previously,[6] and glucopiericidin A (GPA, 10 ng/mL) was used as positive control.[6] Bars, s.d. (n = 3). Data represent three independent experiments.

Further studies of structural modification to develop more potent inhibitors and analysis of structure-activity relationships are now under investigation.

Acknowledgments

This work was supported by a grant from the Ministry of Education, Culture, Sports, Science, and Technology of Japan.

References

1) Deberardinis RJ, Mancuso A, Daikhin E, Nissim I, Yudkoff M, Wehrli S, and Thompson CB, *Proc. Natl. Acad. Sci. USA*, **104**, 19345–19350 (2007).
2) Hsu PP and Sabatini DM, *Cell*, **134**, 703–707 (2008).
3) Madhok BM, Yeluri S, Perry SL, Hughes TA, and Jayne DG, *Am. J. Clin. Oncol.*, in press.
4) Shanmugam M, Mcbrayer SK, and Rosen ST, *Curr. Opin. Oncol.*, **21**, 531–536 (2009).
5) Vander Heiden MG, Christofk HR, Schuman E, Subtelny AO, Sharfi H, Harlow EE, Xian J, and Cantley LC, *Biochem. Pharmacol.*, **79**, 1118–1124 (2010).
6) Kitagawa M, Ikeda S, Tashiro E, Soga T, and Imoto M, *Chem. Biol.*, **17**, 989–998 (2010).
7) Le Clainche C and Carlier M-F, *Physiol. Rev.*, **88**, 489–513 (2008).
8) Molitoris BA, Geerdes A, and Mcintosh JR, *J. Clin. Invest.*, **88**, 462–469 (1991).
9) Witke W, *Trends Cell Biol.*, **14**, 461–469 (2004).
10) Suami T, Lichtenthaler F, and Ogawa S, *Bull. Chem. Soc. Jpn.*, **39**, 170–178 (1966).
11) Ogawa S, Oki S, and Suami T, *Bull. Chem. Soc. Jpn.*, **52**, 1095–1101 (1979).
12) Airley RE and Mobasheri A, *Chemotherapy*, **53**, 233–256 (2007).
13) Mathupala SP, Ko YH, and Pedersen PL, *Oncogene*, **25**, 4777–4786 (2006).
14) Mazurek S, Boschek CB, Hugo F, and Eigenbrodt E, *Semin. Cancer Biol.*, **15**, 300–308 (2005).

Autophagy 7:2, 1-12; February 2011; © 2011 Landes Bioscience

Caffeine induces apoptosis by enhancement of autophagy via PI3K/Akt/mTOR/p70S6K inhibition

Shinji Saiki,[1] Yukiko Sasazawa,[2] Yoko Imamichi,[1] Sumihiro Kawajiri,[1] Takahiro Fujimaki,[2] Isei Tanida,[3] Hiroki Kobayashi,[2] Fumiaki Sato,[4] Shigeto Sato,[1] Kei-Ichi Ishikawa,[1] Masaya Imoto[2] and Nobutaka Hattori[1,*]

[1]Department of Neurology; Juntendo University School of Medicine; Bunkyo, Tokyo; [2]Department of Biosciences and Informatics; Faculty of Science and Technology; Keio University; Kohoku, Yokohama; [3]Department of Biochemistry and Cell Biology; National Institute of Infectious Diseases; Shinjyuku, Tokyo; [4]Research Institute for Disease of Old Age; Juntendo University School of Medicine; Tokyo, Japan

Key words: apoptosis, autophagy, PI3K/Akt/mTOR/p70S6K, ERK1/2, caffeine

Abbreviations: PI3K, phosphoinositide-3 kinase; 4E-BP1, eukaryotic initiation factor 4-binding protein 1; ERK, extracellular signal-regulated kinase; mTOR, mammalian target of rapamycin; 3-MA, 3-methyladenine; MEFs, mouse embryonic fibroblasts; p70S6K, 70-kDa ribosomal protein S6 kinase; PI, propidium iodide; MPP^+, 1-methyl-4-phenylpyridinium

Caffeine is one of the most frequently ingested neuroactive compounds. All known mechanisms of apoptosis induced by caffeine act through cell cycle modulation or p53 induction. It is currently unknown whether caffeine-induced apoptosis is associated with other cell death mechanisms, such as autophagy. Herein we show that caffeine increases both the levels of microtubule-associated protein 1 light chain 3-II and the number of autophagosomes, through the use of western blotting, electron microscopy and immunocytochemistry techniques. Phosphorylated p70 ribosomal protein S6 kinase (Thr389), S6 ribosomal protein (Ser235/236), 4E-BP1 (Thr37/46) and Akt (Ser473) were significantly decreased by caffeine. In contrast, ERK1/2 (Thr202/204) was increased by caffeine, suggesting an inhibition of the Akt/mTOR/p70S6K pathway and activation of the ERK1/2 pathway. Although insulin treatment phosphorylated Akt (Ser473) and led to autophagy suppression, the effect of insulin treatment was completely abolished by caffeine addition. Caffeine-induced autophagy was not completely blocked by inhibition of ERK1/2 by U0126. Caffeine induced reduction of mitochondrial membrane potentials and apoptosis in a dose-dependent manner, which was further attenuated by the inhibition of autophagy with 3-methyladenine or Atg7 siRNA knockdown. Furthermore, there was a reduced number of early apoptotic cells (annexin V positive, propidium iodide negative) among autophagy-deficient mouse embryonic fibroblasts treated with caffeine than in their wild-type counterparts. These results support previous studies on the use of caffeine in the treatment of human tumors and indicate a potential new target in the regulation of apoptosis.

Introduction

Caffeine has a diverse range of pharmacological effects.[1] In addition to its various effects on the cell cycle and growth arrest, higher (4–10 mM) concentrations of caffeine can induce apoptosis in several cell lines, such as 10 mM caffeine in human neuroblastoma cells,[2] 4 mM caffeine in human pancreatic adenocarcinoma cells[3] and 5 mM caffeine in human A549 lung adenocarcinoma cells.[4] Although caffeine has been reported to modulate cell cycle checkpoints and perturb molecular targets of the cell cycle, the exact mechanism of caffeine-induced apoptosis remains unclear.[1]

Autophagy is a key mechanism in various physiopathological processes, including tumorigenesis, development, cell death and survival.[5,6] It has also been shown to have a complex relationship with apoptosis, especially in tumor cell lines.[7] Several reports have shown that autophagy not only enhances caspase-dependent cell death, but is also required for it.[8] In contrast, it has also been shown that autophagy plays an important role in promoting cell survival against apoptosis.[7] Caffeine has been reported to inhibit some kinase activities, including various forms of phosphoinositol-3 kinase and mammalian target of rapamycin (mTOR).[9,10] Recently, in food spoilage studies involving yeast, caffeine has been shown to induce a starvation response,[11] which is a key regulator of autophagy causing its induction. However, the exact mechanism by which caffeine induces autophagy is still unknown.

Here we report that higher concentrations of caffeine enhance autophagic flux in a dose-dependent manner in various cell lines. Furthermore, we show that caffeine-induced autophagy is mainly dependent on PI3K/Akt/mTOR/p70S6 signaling and eventually results in apoptosis.

*Correspondence to: Nobutaka Hattori; Email: nhattori@juntendo.ac.jp
Submitted: 06/22/10; Revised: 10/27/10; Accepted: 11/02/10
Previously published online: www.landesbioscience.com/journals/autophagy/article/14074
DOI:

Results and Discussion

Caffeine (**Fig. 1A**) is a widely used psychoactive drug that has been used for centuries to increase alertness and energy. It has been reported that caffeine induces autophagy in *Zygosaccharomyces bailii* in association with a starvation response, caused by a unknown mechanism.[11] However, it remains unknown whether caffeine affects autophagy in mammalian cells. To determine if caffeine regulates autophagy at a steady state, we first examined levels of the microtubule-associated protein 1 light chain 3 (LC3)-II, which is an LC3-phosphatidyl-ethanolamine conjugate and a promising autophagosomal marker.[12] LC3-II levels (compared to actin loading controls) increased with 5–25 mM caffeine treatment over 48 hours in SH-SY5Y (**Fig. 1B and C**), PC12D and HeLa cells (**Suppl. Fig. S1A and B**). The LC3-II/actin ratio also increased in a time-dependent manner in SH-SY5Y (**Fig. 1D and E**) and HeLa cells (data not shown). Using an electron microscopy technique, the numbers of autophagic vacuoles (AVs) were markedly increased in SH-SY5Y cells treated with 10 or 25 mM caffeine, but not in the control (**Fig. 1F and G**). Morphometric analysis revealed that the number of AVs per 100 μm^2 of SH-SY5Y cytoplasm in control (Mean ± standard deviation: 1.3 ± 0.50), whereas that in caffeine-treated cells (10 mM: 8.0 ± 0.82; 25 mM: 15 ± 1.9) for 24 hours. Expression levels of p62, a well-known autophagic substrate, were also decreased by caffeine treatment in SH-SY5Y (**Fig. 1H and I**) and HeLa cells (**Suppl. Fig. S1C and D**). Furthermore, 10 mM caffeine treatment markedly increased the number of EGFP-LC3-positive vesicles in SH-SY5Y cells transiently transfected with EGFP-LC3 (data not shown) and HeLa cells stably expressing EGFP-LC3 (**Figs. 1J and K**).[12,13] This effect was confirmed by the observation that caffeine administration also increased the number of vesicles positive to endogenous LC3 (**Suppl. Fig. S1E**).

Endogenous LC3 is post-transcriptionally processed into LC3-I, which is found in the cytosol. LC3-I is in turn lipidated to LC3-II, which then associates with autophagosome membranes.[14] LC3-II can accumulate due to increased upstream autophagosome formation or impaired downstream autophagosome-lysosome fusion. To distinguish between these two possibilities, we assayed LC3-II in the presence of E64D plus pepstatin A or bafilomycin A1, which inhibits lysosomal proteases or blocks downstream autophagosome-lysosome fusion and lysosomal proteases, respectively.[15,16] Caffeine significantly increased LC3-II levels in the presence of E64d plus pepstatin A or bafilomycin compared to E64d plus pepstatin A or bafilomycin alone in (**Fig. 2A and B**; **Suppl. Fig. S1F and G**) and HeLa cells (**Fig. 2C and D**; **Suppl. Fig. S1H and I**). A saturating dosage of bafilomycin A1 was used in this assay and no further increases in LC3-II levels were observed when cells were treated with higher concentrations. Similar results were observed in PC12D cell lines (data not shown). To confirm the caffeine effect on autophagic flux, we assessed the numbers of autolysosomes and autophagosomes in HeLa cells. The ratio of the numbers of autolysosomes (positive to both LC3 and LAMP2) to autophagosomes (positive to LC3) was increased by 10 mM caffeine treatment for 48 hours (**Fig. 2E**). Quantification data using ImageJ also showed significant increase of the ratio (**Fig. 2F**). These results strongly indicate that high concentration of caffeine treatment enhances autophagic flux.

The class I phosphatidylinositol 3-phosphate kinase (PI3K)/Akt/mTOR/p70ribosomal protein S6 kinase (p70S6K) signaling pathway and the Ras/Raf-1/mitogen-activated protein kinase 1/2 (MEK1/2)/extracellular signal-regulated kinase 1/2 (ERK1/2) pathway are two well-known pathways involved in the regulation of autophagy. Both are associated with tumorigenesis and often activated in numerous types of tumors.[17] Therefore, we examined the effect of caffeine on both of these pathways, using western blotting, according to the protocol by Inoki and colleagues.[18] After a 24 hour treatment with caffeine, there was a significant decrease in the levels of phosphorylated p70 S6 kinase, S6 ribosomal protein and 4E-BP1, compared with total normal levels in SH-SY5Y (**Fig. 3A**), HeLa and PC12D cells (data not shown). Consistent with these results, nonphosphorylated 4E-BP1 proteins were increased by caffeine treatment (**Fig. 3A**). To further investigate the upstream inhibition of mTOR by caffeine, we examined Ser473 phosphorylation of Akt, which measures both Akt/mTOR and mTORC2 activity. As shown in **Figure 3B**, treatment with caffeine also decreased the level of phosphorylated Akt in SH-SY5Y cells, which was consistent with a previous report.[19] Similar findings were obtained in HeLa (**Suppl. Fig. S2A**) and PC12D cells (data not shown). Subsequently, we examined whether caffeine increases the phosphorylation of ERK1/2, a key regulator of autophagy downstream of Akt. As shown in **Figure 3C**, treatment with caffeine increased phosphorylated ERK1/2. The effects of caffeine on mTOR inhibition were initially detected 3 hours after the addition of caffeine and reached a maximal level after 6 hours in SH-SY5Y (**Fig. 3D**) and 9 hours in HeLa cells (**Suppl. Fig. S2B and C**).

Caffeine has been shown to inhibit PI3K and components of the PI3K/Akt pathway.[9,20] Next, we performed experiments to confirm whether caffeine-induced autophagy is activated through the PI3K/Akt pathway. Insulin or insulin-like growth factor upregulates PI3K and its downstream targets including Akt and mTOR, resulting in the inactivation of autophagy.[21-23] As shown in **Figure 4A and B**, insulin treatment for 30 minutes significantly phosphorylated Akt at Ser473, whereas the phosphorylation was completely abolished by additional treatment with caffeine. No significant differences of the LC3-II/

Figure 1A–G (See opposite page). Caffeine increases autophagic flux in various cell lines. (A) Structural formula of caffeine. (B and C) SH-SY5Y cells treated with various concentrations of caffeine for 24 or 48 hours were analyzed by immunoblotting (B) with antibodies against LC3 and actin. Densitometry analysis of LC3-II levels relative to actin (C) was performed using three independent experiments. (D and E) SH-SY5Y cells treated with 25 mM caffeine for 3–24 hours were analyzed by immunoblotting (D) with antibodies against LC3 and actin. Densitometry analysis of LC3-II levels relative to actin (E) was performed using three independent experiments. (F) Electron microscopic examination of SH-SY5Y cells treated with various concentrations of caffeine for 24 or 48 hours. Autophagic vacuoles accumulating in the cytoplasm are shown by arrows. (G) Morphometric analysis of autophagic vacuoles was performed with 30 different areas of the cytoplasm of control and caffeine-treated cells.

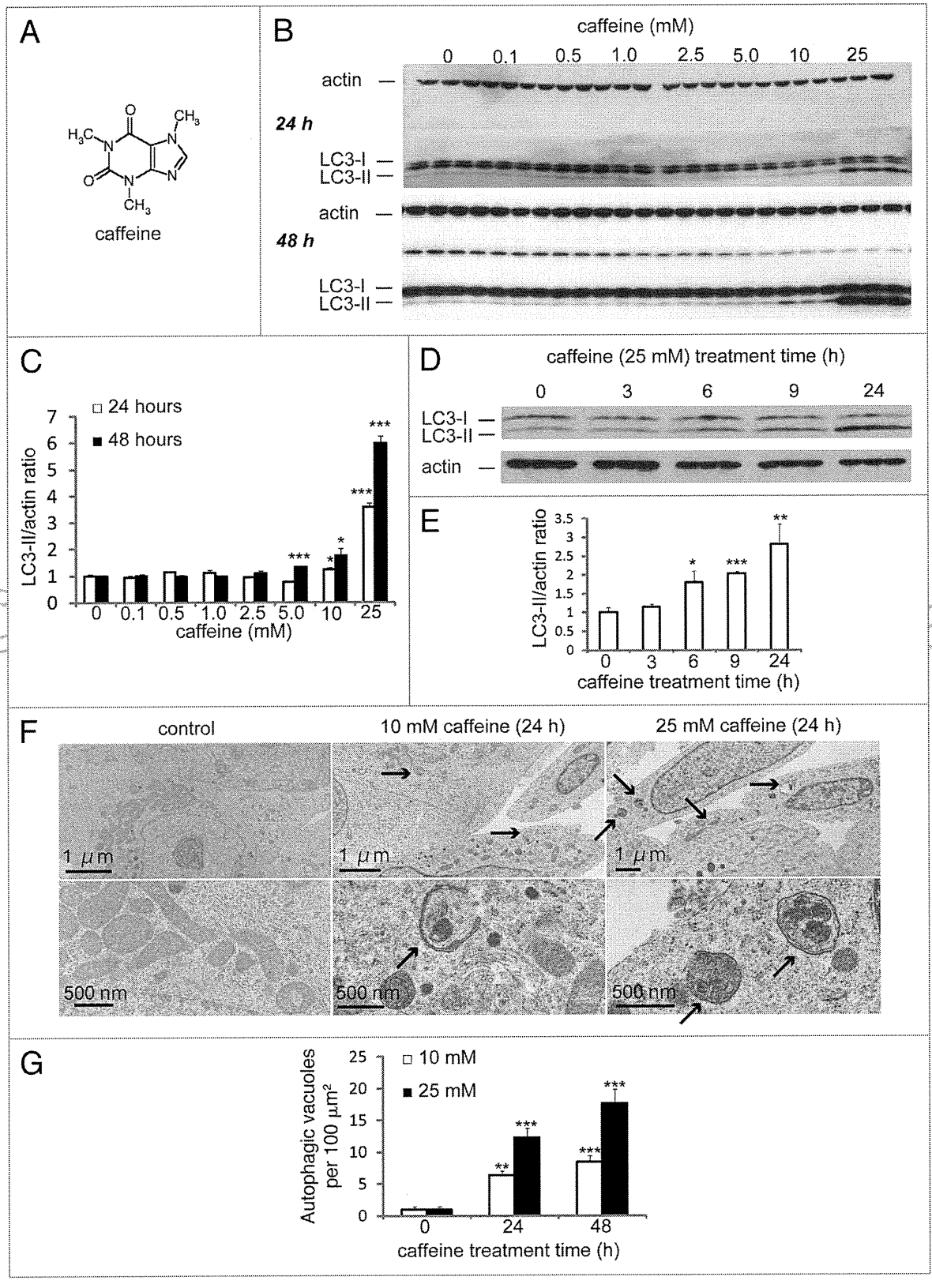

actin ratio between caffeine treatment and caffeine treatment with insulin were observed. Also, caffeine and Akt1/2 inhibitors did not have additive effects on the levels of LC3-II/actin ratio compared to the single treatment of caffeine or Akt inhibitors (**Fig. 4C and D**). To further confirm the caffeine effects on this pathway, cells were transiently transfected with myristoylated Akt (myr-Akt), a constitutively active form of Akt.[24] Caffeine treatment of both cells transfected with control vector and

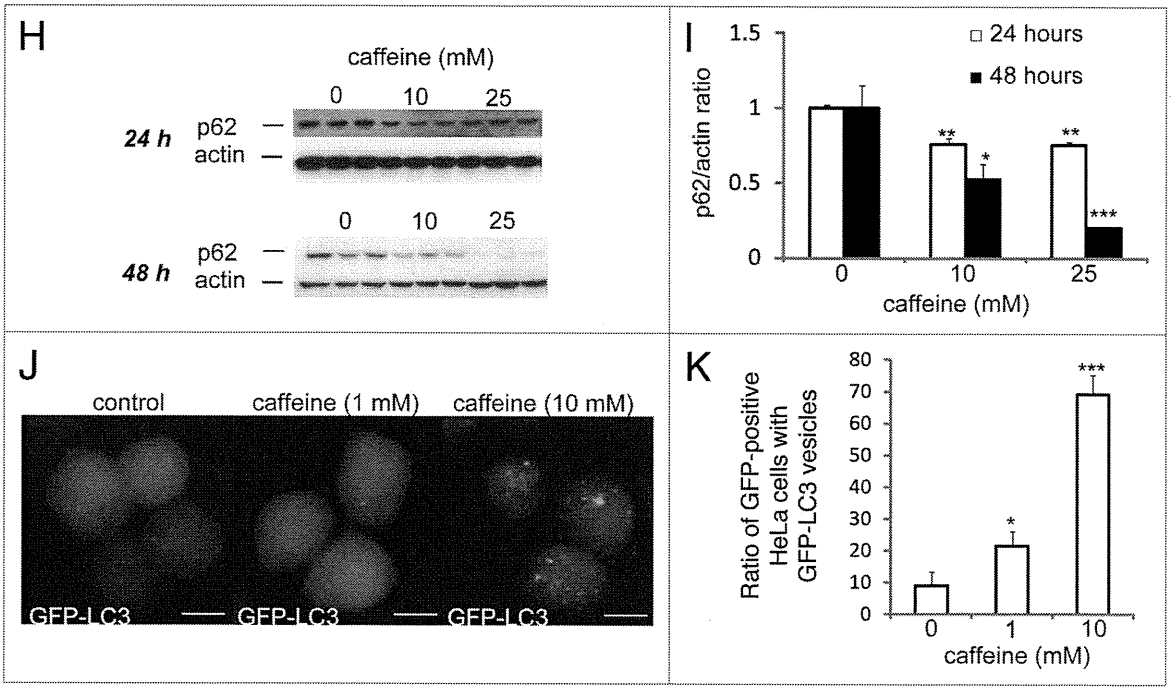

Figure 1H–K. Caffeine increases autophagic flux in various cell lines. (H and I) SH-SY5Y cells treated with various concentrations of caffeine for 24 or 48 hours were analyzed by immunoblotting with antibodies against p62 and actin. Densitometry analysis of p62 levels relative to actin (I) was performed using three independent experiments. (J and K) HeLa cells stably expressing EGFP-LC3 were treated with various concentrations of caffeine for 24 hours and analyzed using confocal microscopy. The percentage of EGFP-positive HeLa cells with >5 EGFP-LC3 vesicles was assessed (K) described previously in reference 43. Error bars, S.D.; *$p < 0.05$; **$p < 0.01$.

myr-Akt markedly decreased the levels of the phosphorylated Akt (**Fig. 3E**), indicating that caffeine directly inhibits the Akt phosphorylation. If caffeine facilitates autophagy through PI3K/Akt and ERK1/2 signalings, the autophagy should be partially blocked by ERK1/2 inhibition using the mitogen-activated protein kinase kinase 1/2 (MEK1/2) inhibitor, U0126. U0126 significantly but mildly reversed the levels of LC3-II/actin ratio (**Fig. 4F and G**). The failure of U1026 to reverse completely the caffeine effect can be explained by the autophagy induction through Akt/mTOR signaling. In addition, only Akt knockdown with inducible short hairpin RNAs (shRNAs) to specifically and stably knock down all three Akt isoforms sufficiently increases autophagic flux.[25] Therefore, we concluded that the caffeine-induced autophagy is mainly dependent on the PI3K/Akt/mTOR pathway.

Because caffeine induces autophagy dependently of mTOR inhibition, we hypothesized that combination treatment of caffeine with rapamycin would not have additive effects on autophagy. However, caffeine and rapamycin showed an additive effect on the enhancement of LC3-II/actin ratio compared to the single treatment of caffeine or rapamycin (**Fig. 5A and B**). Several lines of evidences support the hypothesis that resistance to rapamycin results from a positive feedback loop from mTOR/S6K1 to Akt, resulting in enhancement of Akt phosphorylation at Ser 473.[26-28] Recently, mutual suppression of the PI3K/Akt/mTOR pathway by combination of rapamycin with perifosine, an Akt inhibitor, induces synergistic effects on autophagy-induced apoptosis as well as enhancement of autophagy, suggesting that dual inhibition of the PI3K/Akt/mTOR by rapamycin with caffeine would be also a rational treatment for cancer.[29]

Several anti-cancer agents are known to inhibit the PI3K/Akt/mTOR/p70S6K pathway and simultaneously activate ERK1/2, resulting in induction of autophagy in tumor cell lines.[30,31] The upregulation of this process has beneficial effects in neurodegenerative diseases, such as Parkinson and Huntington diseases, whereas an excess of autophagy can lead to cell death.[32,33] Therefore, we decided to investigate whether caffeine-induced autophagy rescues or induces cell death. Using PC12D cells treated with 1-methyl-4-phenylpyridinium (MPP^+), a well-established Parkinson disease model,[34] we determined that 1 mM caffeine treatment was not sufficient for the induction of autophagy (**Suppl. Fig. S4 and B**) and promoted increased cell viability, whereas >2.5 mM caffeine decreased cell viability (**Fig. 6A**). In addition, a significant decrease in cell viability was noted in cells treated with >2.5 mM caffeine without MPP^+. Also, mitochondrial membrane potentials assessed by JC-1 were significantly preserved by 1 mM caffeine treatment compared to the control with MPP^+, while those were lost by >5 mM caffeine treatment (**Fig. 6B and Suppl. Fig. S5A**). These data suggest that caffeine-induced autophagy is not protective in these cell lines and leads to cell death.

Autophagy and apoptosis may act independently in parallel pathways or may influence one another.[7] To confirm the relationship between these pathways in cells treated with caffeine, we examined caffeine effects on the cell cycle with a propidium iodide (PI) staining assay. Treatment with 2.5–10 mM caffeine

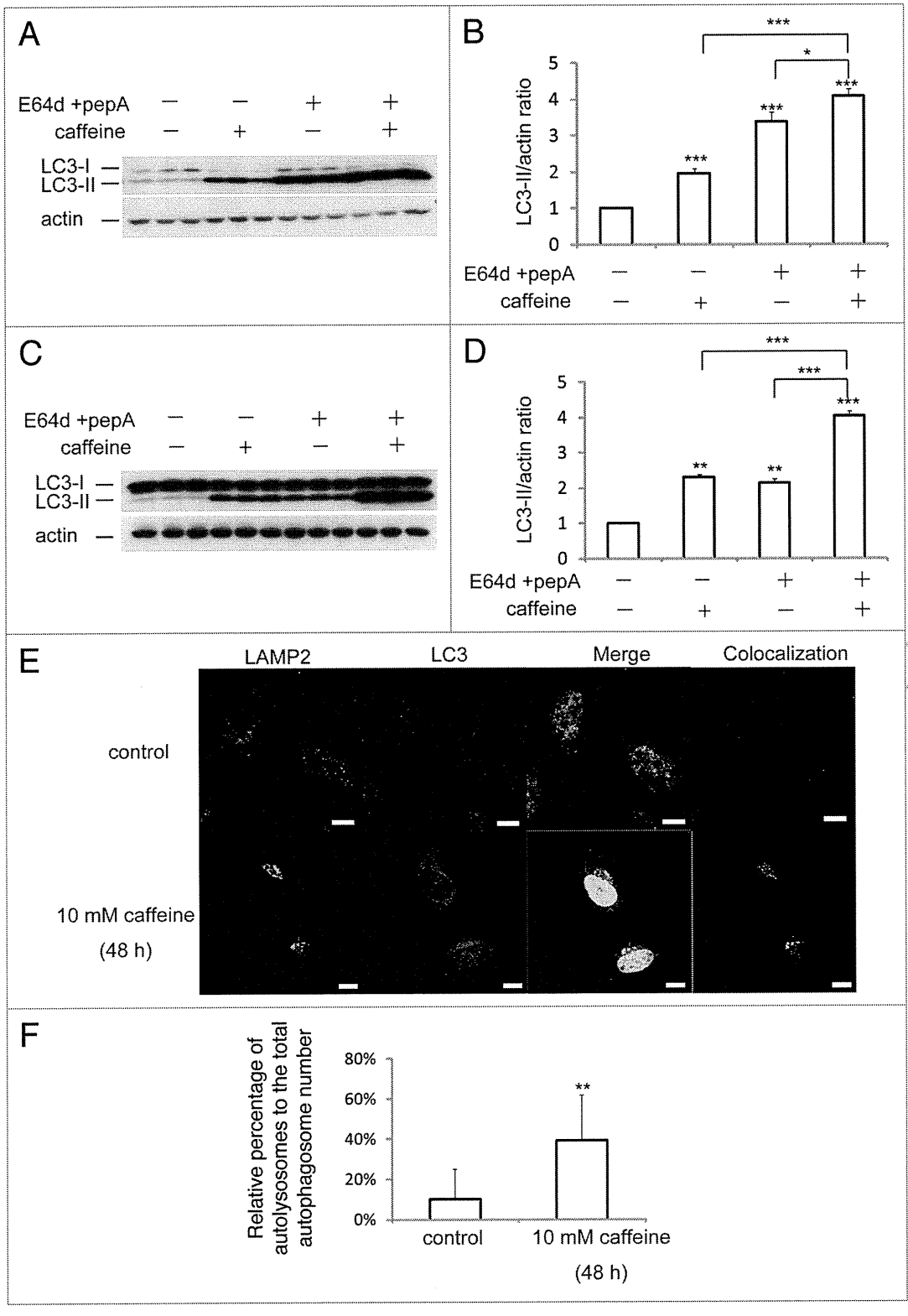

Figure 2. Caffeine does not block autophagosome-lysosome fusion. (A–D) SH-SY5Y (A) or HeLa (C) cells treated with 10 mM caffeine with or without E64d (10 μg/ml) and pepstatin A (10 μg/ml) were analyzed by immunoblotting with antibodies against LC3 and actin. Densitometry analysis of LC3 levels relative to actin in SH-SY5Y (B) and HeLa (D) cells was performed using three independent experiments. (E and F) HeLa cells treated with various concentrations of caffeine for 48 hours were analyzed using confocal microscopy (E). Number of the autolysosomes and autophagosomes were automatically counted using ImageJ "Colocalization" Plugin and the ratios were calculated (F).

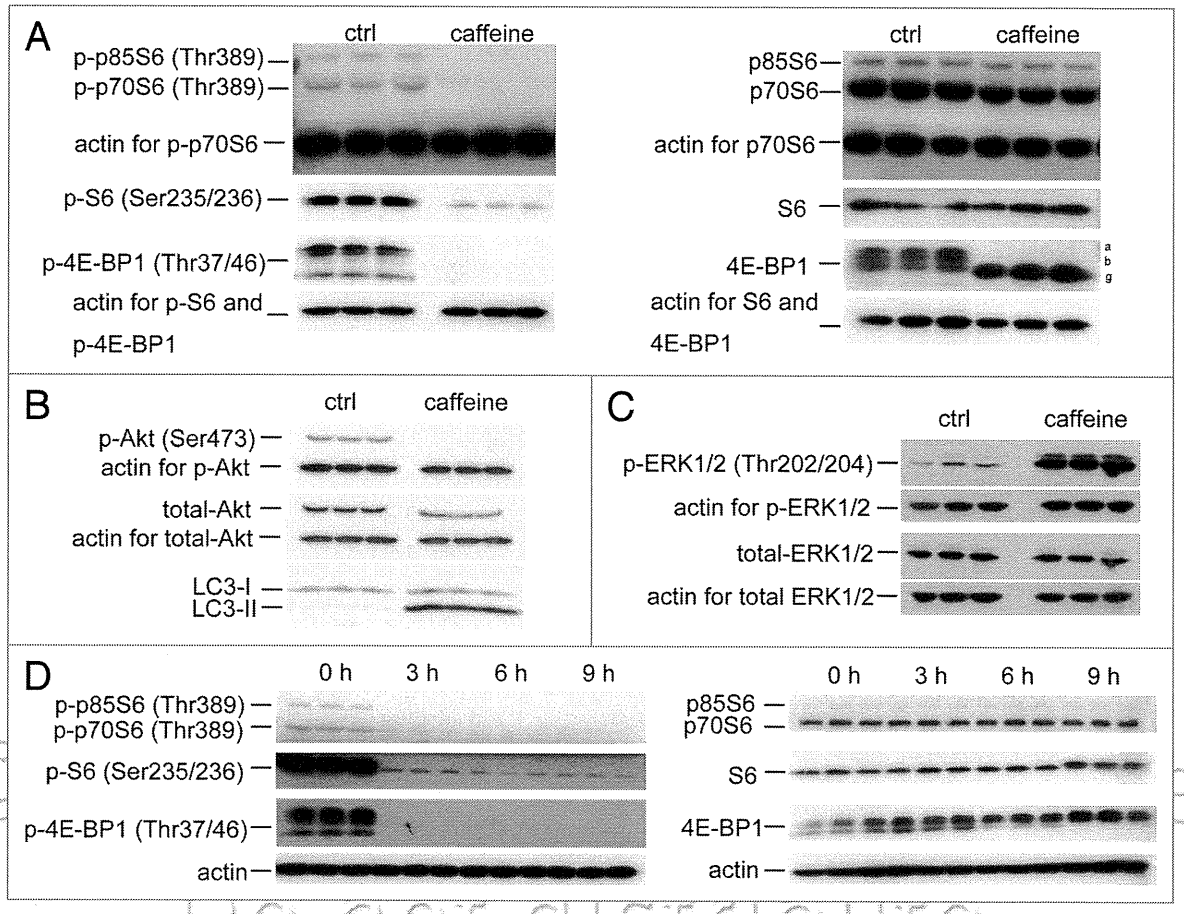

Figure 3. Caffeine inhibits the Akt/mTOR/p70S6 signaling pathway and activates ERK1/2 signaling. (A and B) SH-SY5Y cells treated with or without 10 mM caffeine for 24 hours were analyzed for mTOR activity by immunoblotting for levels of phosphor- and total p70 ribosomal S6 protein, S6, 4E-BP1 (A), Akt (B) and actin. (C) SH-SY5Y cells treated with or without 10 mM caffeine for 0, 3, 6 or 9 hours were analyzed by immunoblotting for levels of phosphor- and total ERK1/2 and actin. (D) SH-SY5Y cells treated with 10 mM caffeine for various time periods were analyzed by immunoblotting for levels of phosphor- and total p70 ribosomal S6 protein, S6, 4E-BP1 and actin.

increased the percentage of cells in the sub-G_1 peak, which is indicative of apoptosis (**Fig. 6C**). To confirm whether caffeine-induced cell death is apoptotic, we examined the activity of caspase-3, a well-known inducer of apoptosis. Treatment with 10 mM caffeine markedly increased levels of cleaved caspase-3 and decreased full-length caspase-3 in PC12D cells (**Fig. 6D**), consistent with previous reports on the induction of apoptosis by caffeine.[35-37]

To test whether caffeine-induced apoptosis is dependent on autophagy, we determined whether the inhibition of autophagy by 3-methyladenine (3-MA) or Atg7 siRNA knockdown affects caffeine-induced cytotoxicity in PC12D cells. Treatment with 1 or 5 mM 3MA or Atg7 knockdown significantly decreased the percentage of cell death or cells with reduced mitochondrial membrane potentials caused by caffeine treatment (5 or 10 mM) (**Fig. 6E and F and Suppl. Fig. S6B**). As can be seen from the increased caffeine-induced apoptosis shown in **Figure 6A and C**, our data suggests that caffeine-induced autophagy is necessary for apoptotic cell death. To further confirm this, we compared autophagy-deficient mouse embryonic fibroblasts (MEFs), lacking the Atg7 gene ($Atg7^{-/-}$), without LC3-II expression (**Suppl. Fig. S4E**), and matched wild-type ($Atg7^{+/+}$) MEFs, in which autophagy is induced by caffeine in a dose-dependent manner (**Suppl. Fig. S4C and D**). As expected, the level of caffeine-induced cell death (positive to trypan blue staining) in $Atg7^{-/-}$ MEFs was less than that in $Atg7^{+/+}$ MEFs (**Fig. 7A**). The numbers of early apoptotic cells (annexin V positive, PI negative) were significantly increased in both a time-dependent and dose-dependent manner by caffeine treatment of $Atg7^{+/+}$ MEFs compared to $Atg7^{-/-}$ MEFs (**Fig. 7B–D**). Also, apoptotic or necrotic cells (annexin V positive) were significantly increased by caffeine treatment of $Atg7^{+/+}$ MEFs compared to $Atg7^{-/-}$ MEFs (**Suppl. Fig. S6**). Together, these results indicate that caffeine-induced autophagy partly occurs upstream of apoptosis and is not a protective response to caffeine.

In various tumor cell lines, higher concentrations of caffeine alone induce p53-dependent G_1 phase arrest and under certain conditions apoptosis can also occur in a p53-independent manner.[1] Furthermore, disruption at the G_2/M checkpoint by caffeine allows cells time to repair DNA damage by driving them through mitosis, eventually resulting in apoptosis.[36,38,39] Consistent with these reports, the results of our study indicate that increased

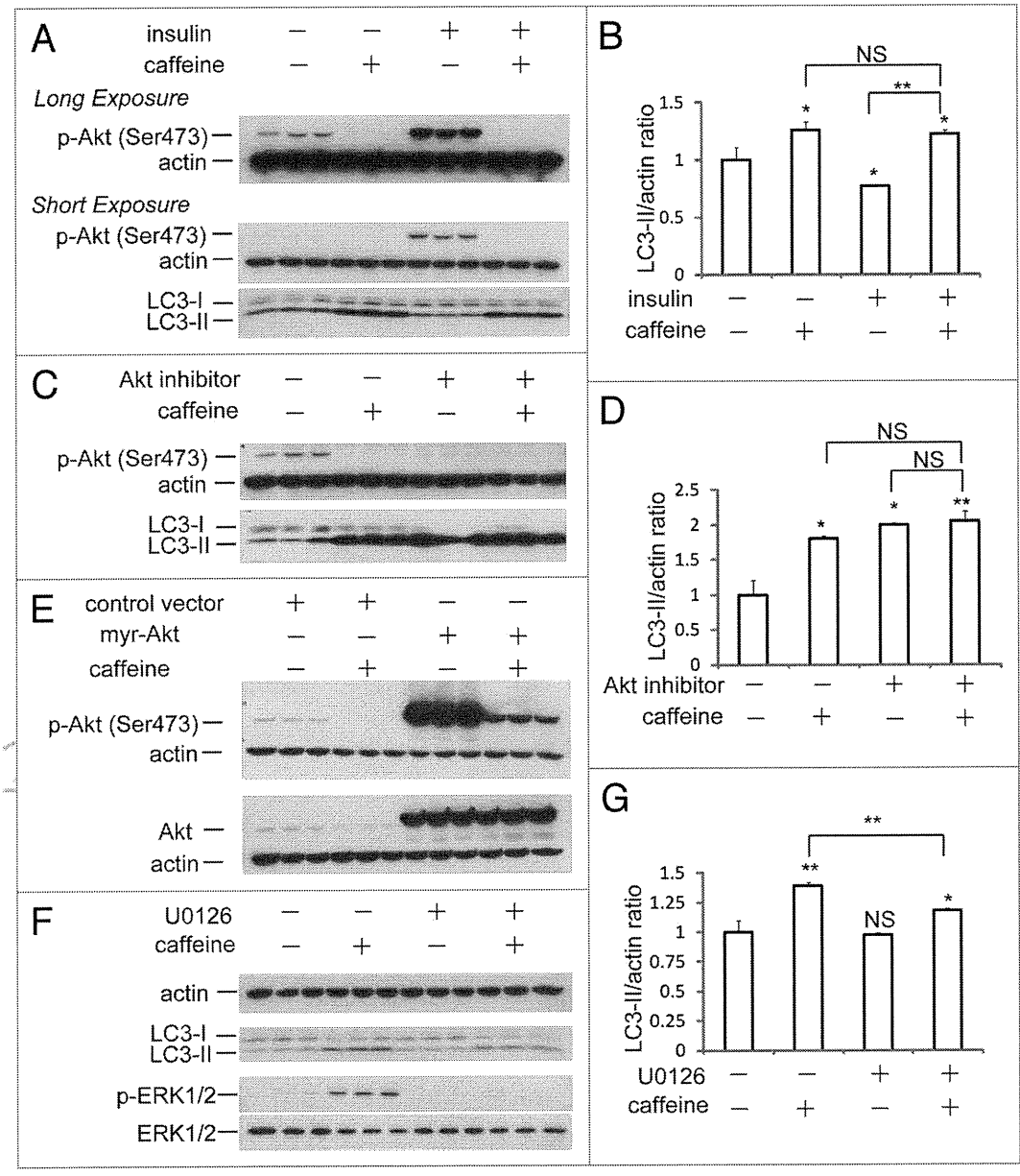

Figure 4. Caffeine-induced autophagy is dependent on PI3K/Akt/mTOR pathway. (A) SH-SY5Y cells treated with 25 mM caffeine for 3 hours followed by treatment with or without 200 nM insulin for 30 minutes were analyzed by immunoblotting. (B) Densitometry analysis of LC3-II levels relative to actin was performed using three independent experiments. (C) SH-SY5Y cells treated with 25 mM caffeine, 50 μM Akt1/2 inhibitors or 25 mM caffeine with 50 μM Akt1/2 inhibitors for 6 hours were analyzed by immunoblotting. (D) Densitometry analysis of LC3-II levels relative to actin was performed using three independent experiments. (E) SH-SY5Y cells were transfected for 24 hours with either a control plasmid DNA (pcDNA3.1) or a plasmid encoding constitutively active Akt (myr-Akt), and then treated with H_2O or 10 mM caffeine for 6 hours. Immunoblotting was performed using antibodies against Akt, p-Akt (Ser 473) and actin. (F) SH-SY5Y cells treated with 25 mM caffeine with or without 20 μM U0126 for 6 hours were analyzed by immunoblotting using antibodies against actin, LC3, p-ERK and ERK. (G) Densitometry analysis was performed using three independent experiments. Error bars, SD; *$p < 0.05$; **$p < 0.01$; N.S., not significant.

concentrations of caffeine treatment cause a dose-dependent increase in apoptosis. More recently, autophagy, a process long known to provide a survival advantage to cells undergoing nutrient deprivation and other stresses, has also been linked to the cell death process.[7] The cross-talk between apoptosis and autophagy is complex and sometimes contradictory; however, it is critical to the overall fate of the cell. In this study, we have shown that autophagy is induced by higher concentrations of caffeine without starvation, mainly via the inhibition of PI3K/Akt/mTOR/p70S6K signaling. Likewise, when caffeine-induced autophagy is blocked by 3-MA treatment or Atg7 knockout, apoptosis is partially attenuated, suggesting that caffeine-induced autophagy occurs upstream of caffeine-induced apoptosis. It also indicates the involvement of other pathways in caffeine-induced apoptosis. These results provide new insight into the effects of caffeine on cell death and survival and its use as a possible